Article:

Zhang, Y., Luo, J., Flewitt, A.J. et al. (2 more authors) (2018) Film bulk acoustic resonators (FBARs) as biosensors: A review. Biosensors and Bioelectronics, 116. pp. 1-15.

https://doi.org/10.1016/j.bios.2018.05.028

Film Bulk Acoustic Resonators (FBARs) as Biosensors: A Review

Yi Zhang[1,2], Jikui Luo[3], Andrew J. Flewitt[4], Zhiqiang Cai[1], Xiubo Zhao[1,2]*

[1]School of Pharmaceutical Engineering and Life Science, Changzhou University, Gehu Road, Changzhou 213164, China

[2]Department of Chemical and Biological Engineering, University of Sheffield, Mappin Street, Sheffield S1 3JD, UK

[3]Institute for Materials Research and Innovation (IMRI), University of Bolton, Deane Road, Bolton BL3 5AB, UK

[4]Electrical Engineering Division, University of Cambridge, JJ Thomson Avenue, Cambridge CB3 0FA, UK

∗Corresponding author: Dr Xiubo Zhao. Tel.: +44 114 222 8256. E-mail: xiubo.zhao@sheffield.ac.uk

Abstract

Biosensors play important roles in different applications such as medical diagnostics, environmental monitoring, food safety, and the study of biomolecular interactions. Highly sensitive, label-free and disposable biosensors are particularly desired for many clinical applications. In the past decade, film bulk acoustic resonators (FBARs) have been developed as biosensors because of their high resonant frequency and small base mass (hence greater sensitivity), lower cost, label-free capability and small size. This paper reviews the piezoelectric materials used for FBARs, the optimisation of device structures, and their applications as biosensors in a wide range of biological applications such as the detection of antigens, DNAs and small biomolecules. Their integration with microfluidic devices and high-throughput detection are also discussed.

Keywords: Film bulk acoustic resonators, FBARs, Biosensors, Biomarkers, Antibodies, Biointerfaces

1. Introduction

Biosensors are analytical devices which combine a biologically sensitive element with a physical transducer to selectively and quantitatively detect the trace of biomarkers such as DNA (Auer et al. 2011; Lin et al. 2010; Nirschl et al. 2009), proteins (Kanno et al. 2000; Nirschl et al. 2009; Quan et al. 2011; Quershi et al. 2009; Sapsford and Ligler 2004; Zhao et al. 2012a), and cells (Ayala et al. 2009). There are different technologies that have been used for biosensors, such as electrochemical impedance spectrometry (EIS) (Ge et al. 2014; Zhu et al. 2014), surface plasmon resonance (SPR) (Cao et al. 2006; Liedberg et al. 1983), micro-cantilever (MCL) (Kim et al. 2003; Lee et al. 2007) and acoustic wave (Flewitt et al. 2015; Guo et al. 2015; Katardjiev and Yantchev 2012; Nirschl et al. 2010; Voiculescu and Nordin 2012). The electrochemical biosensors typically have low sensitivity, while the other two types of technology-based biosensors have very high sensitivity, but are very expensive to manufacture and complex in operation. On the other hand, the acoustic wave-based devices are less expensive without compromising their sensitivity. Bulk acoustic wave (BAW) resonators have been widely employed as sensors for detecting variables such as mass (DeMiguel-Ramos et al. 2017; García-Gancedo et al. 2013; He et al. 2011; Mai et al. 2004; Nagaraju et al. 2014; Qin and Wang 2010; Rey-Mermet et al. 2006), ultra-violet light (Bian et al. 2015), infrared light (Wang et al. 2011a), ozone (Wang et al. 2011b), pressure (Giangu et al. 2015), humidity (Zhang et al. 2015a), volatile organic compounds (Chang et al. 2016; Lu et al. 2015), air pollution (Lee et al. 2015) and biomarkers (Chen et al. 2015b; Dickherber et al. 2008; Guo et al. 2015; Tukkiniemi et al. 2009; Weber et al. 2006; Wingqvist et al. 2008) owing to their high sensitivity, real-time detection, label-free and wireless capabilities (Voiculescu and Nordin 2012). Table 1 compares the mostly reported technologies used in biosensors.

The most commonly reported BAW-based device is the quartz crystal microbalance (QCM). It has two metallic electrodes, usually gold, separated by a quartz crystal. QCMs operating in bulk thickness shear mode are typically used for biosensing applications, and can be used in both wet and dry environments (Fu et al. 2017; Rodahl et al. 1996). The typical resonant frequencies (f_r) of commercially available QCMs are 5, 10 and 20 MHz (Garcia-Gancedo et al. 2011a). QCMs have been used to detect traces of bio-substances in gas and liquid environments for a few decades, providing decent signal strength, excellent temperature stability and sensitivities which can be directly interpreted with the correlation of mass changes. QCMs have also been widely used as biosensors to detect DNA (Caruso et al. 1997; Steichen et al. 2009) and proteins (Corso et al. 2006; Kößlinger et al. 1992; Shons et al. 1972) since 1972, because QCM does not need expensive and/or harmful labels which are usually used in other types of biosensors. However, there are a few drawbacks associated with the QCMs which limit their biosensing applications: (1) large mass detection limit due to the low operation frequency and large base mass; (2) thick substrates (0.5 to 1 mm) and large surface areas (~1 cm^2) which are not ideal for practical applications in terms of cost of sensitivity, operation, scalability and miniaturization; (3) the bulk structure nature of QCMs makes them difficult to integrate with electronics for control, signal read-out, and microfluidic devices, hence limiting their applications as biosensors (Arce et al. 2007; Kanazawa 1997; Marx 2003).

In the last decade, film bulk acoustic resonators (FBARs), a member of the family of BAW-based devices, have been increasingly used as sensors for biological analysis and medical diagnostics, such as cancer, cardiovascular disease, and hypertension (Fu et al. 2010; Hirsh 2006; Nirschl et al. 2010; Xu et al. 2012) on account of their inherent advantages such as ultra-high sensitivity, small size, simple operation and low fabrication cost (Khanna et al. 2003; Krishnaswamy et al. 1990). Unlike QCMs, FBARs use piezoelectric thin films instead of bulk crystals as the transduction material. Because these piezoelectric films are much thinner than those quartz crystals used in QCMs, FBARs have much higher f_r and smaller base mass, hence much higher sensitivity than those of QCMs. Moreover, piezoelectric thin films have good adherence and can be grown on various substrates such as silicon, glass, and polymer films, making them convenient for integrating with microfluidic devices to realize the lab-on-a-chip applications (Garcia-Gancedo et al. 2010a; Garcia-Gancedo et al. 2011a; García-Gancedo et al. 2011b; Kim et al. 2013; Zhang et al. 2014a), and with complementary metal oxide semiconductor (CMOS) electronics for measurement control and signal acquisition and processing. In this paper, we will review the technology of FBARs, their applications as biosensors with focus on immunosensors, and their integration with microfluidics.

Table 1. Comparison of mostly reported technologies for biosensors.

Platform		Detection principles	Measuring parameter /magnitude		Typical LOD and/or sensitivity, and/or linear range	Applications	Ref.
SPR*		Based on the changes in the reflected light obtained on a detector	Refractive index		On the order of 10 pg/ml	Detection of binding kinetics and affinity, such as DNAs, RNAs, proteins, carbohydrates, lipids, and cells	(Islam et al. 2011; Nguyen et al. 2015; Singh 2016; Wijaya et al. 2011)
EIS*		Based on the changes of the charge transfer resistance (R_{ct}) using a redox couple	Charge transfer resistance		0.01 – 100 ng/ml	Proteins, antigen-antibody, cells, DNAs, viruses	(Hu et al. 2013; Manickam et al. 2012; Ohno et al. 2013)
MCL*		Based on the changes in the deflection response or vibrating frequency	Displacement or resonant frequency		A few ng/ml to µg/ml	Cells, viruses, interactions, DNA hybridization, enzymes	(Hansen and Thundat 2005; Xu et al. 2014)
SAW*		Based on the changes of electrical response altered by any material changes at the surface of the sensor		a few MHz – GHz	A few µg/ml to mg/ml	Proteins, antigen-antibody, DNAs, bacteria, ligands	(Flewitt et al. 2015; Lee et al. 2011; Liu et al. 2016)
BAW*	QCM	Based on the resonance frequency altered by the adsorption of a thin layer of material on the electrodes' surface	Resonance frequency	5 – 20 MHz	~10 ng/cm^2 (1 ng/cm^2 is possible with improved fabrication)	Peptides, proteins, oligonucleotides, bacteriophages, viruses, bacteria, cells, DNAs	(Gabl et al. 2004; Montagut et al. 2011)
BAW*	FBAR	Based on the resonance frequency altered by the adsorption of a thin layer of material on the electrodes' surface	Resonance frequency	2 – 10 GHz	A few ng/cm^2	Antigen-antibody, DNAs, ligands, cells	(Chen et al. 2011; Nirschl et al. 2009; Xu et al. 2011)

*: SPR = Surface Plasmon Resonance; EIS = Electrochemical Impedance Spectroscopy; MCL = Micro-cantilever; SAW = Surface Acoustic Wave; BAW = Bulk Acoustic Wave.

2. Film bulk acoustic resonators (FBARs)

2.1. Theory of FBARs

FBAR is one of the BAW-based microelectromechanical devices which has a similar structure to a QCM, and its working mechanism and operation are also based on the same principle. As mentioned above, the main differences between a QCM and a FBAR are the thickness, size and nature of the transduction material which is sandwiched between the two metallic electrodes. Instead of the quartz crystal being employed in a QCM, piezoelectric thin films are used as the transduction material in FBARs. Figure 1 schematically shows the cross-section of an FBAR with a back-trench structure used in our previous work. Compared with quartz crystals, piezoelectric thin films, typically zinc oxide (ZnO) and aluminium nitride (AlN), possess favoured piezoelectric properties such as high electro-mechanical coupling coefficient (k^2), high acoustic velocity, and low acoustic loss (Flewitt et al. 2015; Garcia-Gancedo et al. 2010b). Combination of these properties with thin films in the thickness of a few micrometres results in FBARs with very high f_r from sub-GHz to 10 GHz and high quality factor (Q).

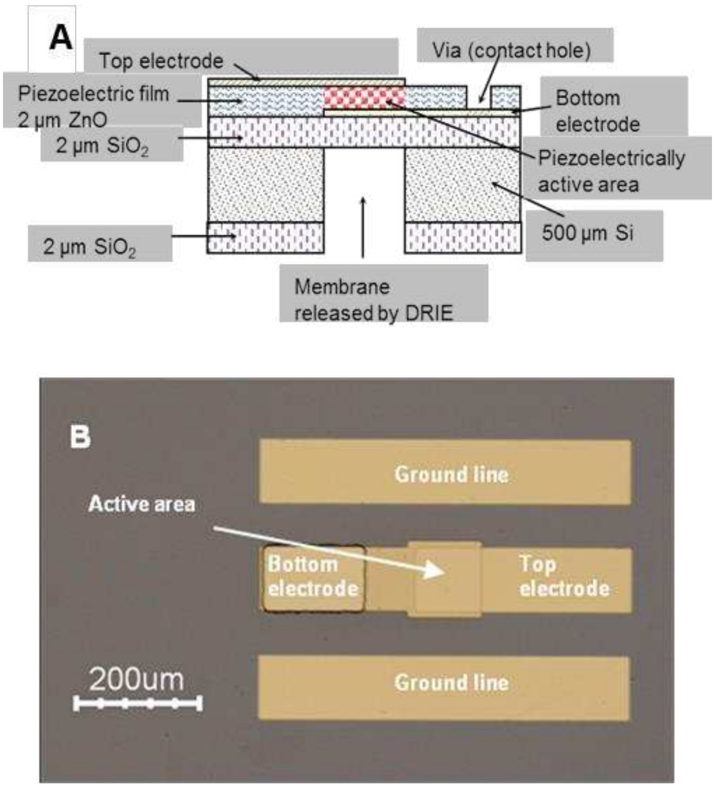

Figure 1. (A) A schematic cross-sectional view of a designed FBAR. (B) Top view of the fabricated FBAR devices (Zhao et al. 2012a). (Copyright © 2012 Elsevier Ltd.)

For the FBARs to be operational on a substrate, the active area of an FBAR must be isolated from the substrate completely, otherwise the acoustic waves generated by the piezoelectric film will radiate into the substrate, leading to no standing waves, hence no resonance. There are two basic types of FBAR device structures. The first is a solidly mounted resonator (SMR) that is formed by isolating the resonator from the substrate with an acoustic Bragg reflector as shown in Figure 2A (DeMiguel-Ramos et al. 2014; Kim et al. 2012). The other is an air-cavity resonator (Figure 2B) which can further be divided into three sub-categories: back-trench type, air-cavity types with cavity either etched into or on the substrate (Lee et al. 2015). The Bragg mirror layer and air-cavity act as effective reflectors so that standing waves can be formed between the two metallic electrodes, and the FBARs can be operated at the resonant frequencies. Recently, a new type of FBAR structure has been developed by utilizing a polymer layer with very low acoustic impedance as the acoustic reflector, and the FBARs can be made on any solid substrate such as glass and copper film even with uneven surfaces (Chen et al. 2015a).

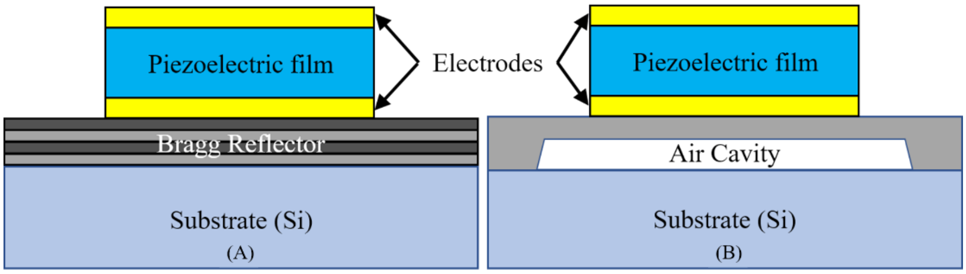

Figure 2. Two types of FBAR structures. (A) A schematic of a solidly mounted resonator (SMR); (B) A schematic of an air-cavity resonator.

There are two basic resonant modes operated in FBARs: (1) longitudinal mode which is a longitudinal acoustic standing wave generated between two surfaces of the electrodes when an alternating voltage is applied (Fu et al. 2010; Lin et al. 2011; Zhang et al. 2010); (2) thickness shear mode which is a shear wave generated between two electrodes with applied alternating electric field. The key difference of these two modes lies in the *c*-axis angle of the crystal columns of the piezoelectric films. In the fabrication of a longitudinal mode FBAR, the piezoelectric film has a crystal orientation normal to the film plane or substrate (Figure 3A), whereas a shear mode FBAR consists of a piezoelectric material with off *c*-axis crystal orientation (Figure 3B). For example, it has been reported that an FBAR device with a 34.5° *c*-axis tilted piezoelectric thin film produces strong shear mode transmittance (Qin et al. 2010). Experiments have been carried out to investigate the mass detection in air and in liquid using both longitudinal mode and shear mode FBARs. As shown in Figure 3C, the longitudinal mode waves of the FBAR almost disappears in a liquid environment because of severe damping of resonant waves in liquid (accompanied with severe decrease of Q), which reduces the mass resolution and sensitivity substantially, whereas the shear mode waves travel in plane with little damping in liquid, hence the FBAR maintains high Q and sensitivity. Therefore, the former mode can only work under dry condition, while the latter is able to work in both dry and liquid environments (Rughoobur et al. 2017; Rughoobur et al. 2016). Most of the biosensing applications require the measurements to be carried out in liquid environments to maintain the integrity of the living bio-substances, hence, the shear mode FBARs are more suitable for biosensing applications (Fu et al. 2010).

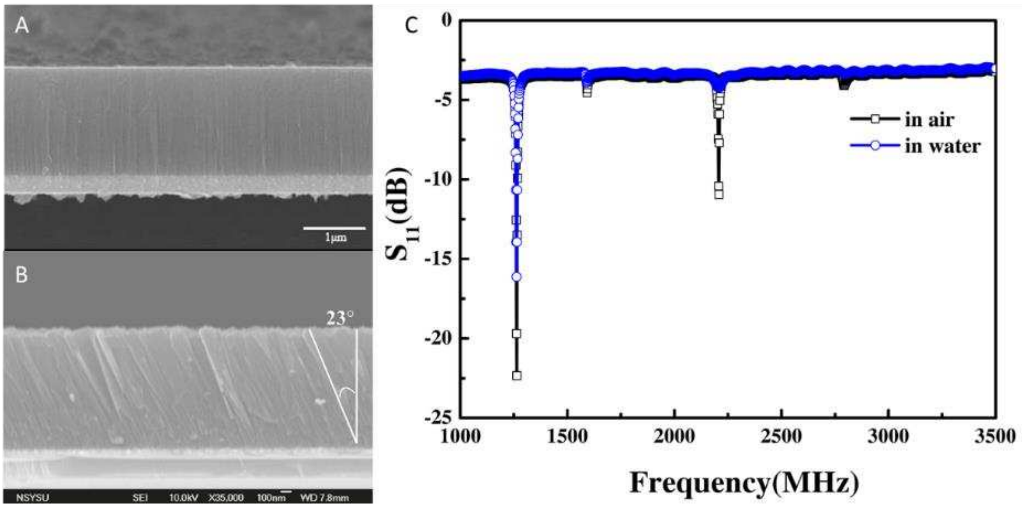

Figure 3. SEM images of cross-sectional views of aluminium nitride (AlN) thin films. (A) A preferred *c*-axis orientation for longitudinal mode FBAR. The preferred orientation of the polycrystalline film was with the *c*-axis of the hexagonal AlN perpendicular to the substrate surface and has better piezoelectric characteristics (Lee and Song 2010). (Copyright © 2010 Elsevier Ltd.) (B) A inclined AlN film for shear mode FBAR. The *c*-axis of the hexagonal AlN columns has a titled angle which enables the sensor excitation of the shear mode wave and is appropriate for the applications in liquid conditions (Chen et al. 2015b). (Copyright © 2015 Chen et al.; licensee Springer) (C) The frequency response of a FBAR device in air and liquid environments, indicating the loss of longitudinal mode at 2.2 GHz when measured in a liquid environment (Chen et al. 2015b). (Copyright © 2015 Chen et al.; licensee Springer)

The classic applications of FBARs as sensors are for gravimetric measurements (Lin et al. 2008b; Qin and Wang 2010; Wingqvist 2010). It is well known that the f_r decreases when an additional mass is added to the resonator's surface (Fanget et al. 2011; Gabl et al. 2004). Therefore, the mass changes can be measured by monitoring the change in f_r. An explicit relationship between the additional mass and frequency shift was developed by Sauerbrey in 1959 for resonators as shown in the following equation (Sauerbrey 1959).

$$\Delta \mathrm{f} = -\frac{2\,\mathrm{f}_\mathrm{r}^\mathrm{n}}{\mathrm{A}\sqrt{\rho_\mathrm{q}\mu_\mathrm{q}}}\Delta \mathrm{m} \qquad \text{(Equation 1)}$$

Where Δf is the frequency change (Hz), f_r is the resonant frequency (Hz), Δm is mass change (g), A is the piezoelectrically active area (cm^2), ρ_q is the density of piezoelectric material (g/cm^3), and μ_q is the shear modulus of piezoelectric material (g·cm^{-1}·s^{-2}), n is a number between 1 and 2. The equation was developed for correlating the changes in f_r of a piezoelectric material with the additional mass deposited on it, treating the deposited mass as an extension of the thickness of the piezoelectric material. This allows the small additional mass to be determined without calibration. This theory also applies to FBAR resonators for biosensing, but with modified numerical number, n, typically $1 < n < 2$. The f_r of an FBAR device is correlated with the acoustic velocity, v_s, by $f_r = v_s/2h$, here h is the thickness of the piezoelectric film, thus it can be adjusted by the thickness of the piezoelectric thin films once the piezoelectric material to be used is determined (Garcia-Gancedo et al. 2011a). The thicknesses of the piezoelectric thin films used in FBARs are commonly in sub-micrometre to a few micrometres, resulting in f_r ranging from a few GHz to a few hundreds of MHz (Gao et al. 2016; Katardjiev and Yantchev 2012; Zhao et al. 2014). From equation 1, it is clear that the sensitivity of a resonator is proportional to the f_r of the device, inversely proportional to the active area or base mass, and these are the reasons why FBARs have higher sensitivities than those of QCMs and SAW devices.

The quality factor (Q) of a resonator is a dimensionless parameter that describes how underdamped a resonator is, and characterizes a resonator's bandwidth relative to its centre frequency. The standard definition is shown by the following equation (Rughoobur et al. 2017):

$$Q = \frac{f_r}{2}\left|\frac{d\Phi_Y}{df}\right|_{f=f_r} \qquad \text{(Equation 2)}$$

where f_r is the resonant frequency and Φ_Y is the phase of the electrical admittance. FBARs with high Q values have sharper resonant peaks than that of FBARs with lower Q values, and are more accurate in monitoring small frequency shifts, resulting in higher sensitivities. Therefore, the sensitivity of FBARs is mainly determined by both f_r and Q.

FBAR is excited by applying a microwave (RF) signal on the electrodes of the device, hence its performance is significantly influenced by the electromechanical coupling coefficient (k^2). k^2 is a measure to indicate how much of the applied energy being coupled to the device and is expressed as equation 3.

$$k^2 = e_{31}^2 / (c_{11} \cdot \varepsilon_{33}) \qquad \text{(Equation 3)}$$

Where e_{31}^2 is the electric field, C_{11} is the elastic constant, and ε_{33} is the permittivity of the material. k^2 depends on the piezoelectric properties of the material used and the wavelength of the device. As there are many factors such as electrodes and loss in the piezoelectric thin film affecting the electromechanical coupling coefficient of a FBAR, the most commonly used term for the assessment is the effective electromechanical coupling coefficient, k_{eff}^2, which is expressed as follows (Chen and Wang 2005).

$$k_{eff}^2 = \frac{\pi^2}{4}\left(\frac{f_p - f_s}{f_p}\right); \text{ or } k_{eff}^2 = \frac{f_p^2 - f_s^2}{f_p^2} \qquad \text{(Equation 4)}$$

Where f_s and f_p are the series and parallel resonance frequencies, respectively. Similar to other acoustic resonators, k_{eff}^2 for FBARs is relatively small values, mostly less than 10%.

Temperature has significant effects on performance and characteristics of FBAR biosensors, therefore temperature calibration is needed for precise detection and determination of bio-analytes. Temperature dependency of FBAR frequency is mainly caused by variation of acoustic velocity, thermal expansion of piezoelectric material etc. Their relationships are expressed as following (Fu et al. 2017):

$$TCF = \frac{1}{f_o}\frac{df}{dT} = \frac{1}{v}\frac{dv}{dT} - \frac{1}{L}\frac{dL}{dT} = \frac{1}{v}\frac{dv}{dT} - \alpha \qquad \text{(Equation 5)}$$

TCF can be determined experimentally using:

$$TCD = \frac{1}{f_o}\frac{f - f_o}{T - T_o} \qquad \text{(Equation 6)}$$

Where f and f_0 are the resonant frequencies at temperatures of T and T_0. For most of FBARs, the frequency is linearly correlated to temperature, thus by measuring the frequencies as a function of temperature, the *TCF* values can be easily determined experimentally. For precision bio-detection, the TCF of the FBAR needs to be determined, and the measurement results are to be calibrated by temperature measured by an additional temperature sensor. Recently, a simple self-temperature calibrated method has been developed for FBAR and acoustic resonator sensors (Gu et al. 2018; Liu and Flewitt 2014; Xu et al. 2018). Most of FBARs with a support membrane have dual wave modes, and they have different sensitivities to temperature and analyte. This can be utilized for decoupling the temperature effect from the bio-detection. If the f_r of both wave modes, mode 1 and mode 2, are linear function of temperature and additional mass, and the mass sensitivities are as α_1 and α_2, and the temperature sensitivities are β_1 and β_1, respectively, then the total frequency shift for the mode 1 and mode 2 are expressed as following (Xu et al. 2018):

$$\begin{cases} \Delta f_{M1} = \alpha_1 \varepsilon + \beta_1 T \\ \Delta f_{M2} = \alpha_2 \varepsilon + \beta_2 T \end{cases}, \qquad \text{(Equation 7)}$$

Where ε is the additional mass, T is temperature, Δf_{M1} and Δf_{M2} are the frequency shift of mode1 and mode2 resonant peaks, respectively. Then, we can obtain

$$\begin{cases} \varepsilon = (\beta_2 \Delta f_{M1} - \beta_1 \Delta f_{M2})/(\beta_2 \alpha_1 - \beta_1 \alpha_2) \\ T = (\alpha_2 \Delta f_{M1} - \alpha_1 \Delta f_{M2})/(\beta_1 \alpha_2 - \beta_2 \alpha_1) \end{cases}, \qquad \text{(Equation 8)}$$

thus, the additional mass of the bio-substances and temperature can be measured simultaneously, or the mass measured being calibrated with temperatures.

2.2. Piezoelectric films employed in FBARs

The quality of the piezoelectric thin films plays a vital role in FBARs' performances. In order to fabricate a high-quality FBAR, several requirements are desired for the piezoelectric films to be used in FBARs: (1) highly organized microstructures, e.g. high crystallinity with preferred *c*-axis orientations or off *c*-axis orientation with certain angle for shear mode; (2) good piezoelectric properties; (3) high electromechanical coupling coefficient k^2; (4) easy fabrication process and low cost; (5) good biocompatibility for use as biosensors (Fu et al. 2010; Kang et al. 2005).

A variety of piezoelectric materials such as zinc oxide (ZnO), lead zirconate titanate (PZT), aluminium nitride (AlN), gallium arsenide (GaAs) and polyvinylidene fluoride (PVDF) have been used in FBARs (Bjurstrom et al. 2006; DeMiguel-Ramos et al. 2017; DeMiguel-Ramos et al. 2014; Kim et al. 2003; Lin et al. 2008c; Mai et al. 2004; Qiu et al. 2011; Sapsford and Ligler 2004). Each of them has strengths and weaknesses. For example, PZT has a unique range of properties such as very high piezoelectric constant and k^2, but also has disadvantages such as higher acoustic wave attenuation, lower sound wave velocities, difficulty in making thick films for FBARs and poor biocompatibility which limit its applications as biosensors (Fu et al. 2010). GaAs, SiC and PVDF films are relatively less popular than other piezoelectric films as they are either expensive or have poor piezoelectric properties. Other piezoelectric thin films have also been explored such as Barium strontium titanate (BST) and Gallium nitride (GaN) for the fabrication of FBARs, with the focus mostly on the high frequency for application in communication (Koohi and Mortazawi 2017; Muller et al. 2009). Piezoelectric AlN thin films have high phase velocity, particularly useful for high f_r FBARs, favoured hardness and chemical stability. However, the fabrication process of AlN films is more difficult than other piezoelectric films such as ZnO (Gao et al. 2016), and also AlN film's k^2 is relatively small compared to that of ZnO devices. ZnO film exhibits good piezoelectric properties and high k^2, and has a high controllability of the film stoichiometry, texture and other properties during fabrication process. Moreover, ZnO is highly biocompatible which is suitable for bio-applications. Therefore, ZnO film is the most commonly used piezoelectric thin film in fabrication of FBARs (Dickherber et al. 2008; Flewitt et al. 2015; Garcia-Gancedo et al. 2011a; Singh et al. 2011; Yakimova et al. 2012). However, ZnO is not a CMOS compatible material and cannot be used in modern microelectronic manufacturing factories, limiting its mass production and widespread applications. Nevertheless, AlN and ZnO are two of the mostly used piezoelectric materials for fabricating FBARs, and the choice between either using AlN or ZnO depends on the fabrication conditions and applications.

A number of methods including chemical vapour deposition (CVD), sol-gel method and sputtering have been adopted to deposit piezoelectric films on support substrates. Of these, sputtering has been widely employed to deposit piezoelectric films, mostly ZnO and AlN, onto a variety of electrodes for the fabrication of FBARs. There are different types of sputtering, such as high target utilisation sputtering (HiTUS), RF magnetron sputtering, and reactive sputtering. Generally, the piezoelectric films deposited by sputtering possess good crystallographic orientation, high packing density, high resistivity (> 10^9 MΩ for HiTUS), and superior adhesion to substrates (Garcia-Gancedo et al. 2010b; Kang et al. 2005). Those properties are significantly affected by the sputtering process parameters such as the type of substrates (Kang et al. 2005), the input power (Jun Phil et al. 2003), deposition temperature, and the sputtering gas pressure etc. (Lee et al. 2003).

2.3. Optimisation of FBARs

There have been many reports on improving the sensitivity of FBAR sensors, including optimising the device structures, choice of piezoelectric thin films and electrode materials, and the fabrication processes of piezoelectric thin films or/and modifying the electrodes to achieve high-quality signal responses. Electrodes are necessary for the fabrication of FBARs, however the properties of the electrode materials affect the performance of the FBAR significantly, thus the choice of materials for the electrodes is important. Materials with high conductivity, low mass density and high elastic modulus, high acoustic impedance mismatch with the piezoelectric thin film or substrate are essential for high performance FBARs. Electrode materials with high mass density reduce the quality factor as it is part of the mass loading, whereas "soft" materials such as Al has low acoustic impedance, not particularly suitable to be the electrode materials for high quality FBARs. From these aspects, the best materials for the electrodes of FBARs are the carbon-nanotubes which has the lowest mass density, highest elastic modulus (Garcia-Gancedo et al. 2011a). Dragoman et al. (Dragoman et al. 2006) found that Coating the metal electrode surface of GaN based FBARs with a mixture of carbon-nanotubes (CNT) network could effectively increase the quality factor by more than ten times, mostly attributed to the improved elastic modulus of the combined top electrode. García-Gancedo et al. (Garcia-Gancedo et al. 2010a; Garcia-Gancedo et al. 2011a) further developed high performance FBARs with a thermally-grown CNTs only top electrode, and found the FBARs have a much higher Q (> 2000) compared with those using standard metal electrodes and CNT/metal composite electrodes. Recently, Esconjauregui et al. (Esconjauregui et al. 2015) have also demonstrated that growth of carbon nanotube forests on piezoelectric AlN films as the top electrode material can significantly improve the performance of FBAR devices. CNTs top electrodes not just improve FBARs' performances, but also provide much enhanced binding sites for biological reaction, hence improving biosensor sensitivity. Theoretically, multilayer graphene sheets would be another fantastical electrode material for fabricating high Q FBARs, many attempts, including the authors', to fabricate such devices, it is yet to be realized. Meanwhile, it has also been shown that a micro through-hole array in the top electrode provided paths for gas to reach the sensitive layer directly and improved the sensitivity of the FBARs (Zhang et al. 2015a).

Material properties of the piezoelectric thin films influence the performance of FBAR markedly as they determine the quality factor (Q), coupling coefficient etc. ZnO and AlN are the two mostly used piezoelectric thin films owing to their easy deposition and high-quality crystallinity etc. Garcia-Gancedo et al. (Garcia-Gancedo et al. 2010b) reported that the morphological and electro-acoustical properties (e.g. the crystalline orientation, surface morphology and electrical resistivity) of the thin film are of great importance to a successful FBAR with a high f_r. ZnO thin films normally have smoother surfaces and high piezoelectric constant than those of AlN ones, and easy to synthesize. AlN has high acoustic velocity and is biocompatible with high chemical inertness, particularly suitable for biosensor applications, but its piezoelectric constant and coupling coefficient are not as good as those of ZnO. To this end, a new type of piezoelectric material AlScN doped with scandium up to 40% has been developed, which showed much improved effective electromechanical coupling coefficient by 300 – 400% (Akiyama et al. 2009; Wang et al. 2014b) and has been used to fabricate FBARs with coupling coefficient of the device up to 3.8% achieved (Pashchenko et al. 2016). Additionally, the thickness of piezoelectric films can be optimised depending on the electrode materials has been reported (Choi et al. 2014).

Performances of the FBARs can be adjusted by the device design parameters. The finite element method (FEM) was employed to study the effects of electrode variations on k^2. The results showed that the design parameters such as electrode material, electrode configuration and electrode area have significant effects on the k^2. For example, in order to fabricate FBARs with high k^2, high acoustic impedance electrodes and optimised thickness ratio of electrode/piezoelectric films are crucial to the design. Besides, FBARs with square or rectangle top electrodes have higher k^2 than FBARs with triangle or arbitrary quadrilateral top electrodes (Zhang et al. 2014c). Zhang et al. (Zhang et al. 2014b; Zhang et al. 2015b) demonstrated that a hydrophobic Teflon film covering the non-sensing area of the FBARs can improve the limit of detection significantly. The hydrophobic Teflon film coating not only reduces the required sample volume but also blocks the physical adsorption of target molecules on non-active areas, therefore, improving the adsorption/binding kinetics. Meanwhile, Liu et al. (Liu et al. 2015) recently demonstrated that the f_r of an individual FBAR device can be tuned by coating polymeric layers (poly(acrylic acid) (PAA) and poly(4-vinylpyridine)(PVP)) on top of the devices through either dipping or spin coating method. A maximum f_r shift of more than 20 MHz can be achieved. Furthermore, Chen et al. (Chen et al. 2015a) recently reported that FBAR devices can be integrated on arbitrary substrates using a polymer support layer, making it possible for integrating FBAR sensors onto a variety of substrates, therefore enabling wider applications.

3. FBARs as biosensors

3.1. FBARs as protein biosensors

One important type of protein biosensors is the immunosensors. Immunoassays are biochemical tests that measure the presence or concentration of an analyte (usually antigen) in a biological solution (e.g. serum, urine) by using antibody – antigen interaction. They can qualitatively and quantitatively detect analytes, which provide a reliable and efficient analysis. As such, immunosensors have been increasingly applied to medical diagnosis, drug development, crime detection etc. The classic detection model is to use immobilized antibodies to capture antigens. For example, a prostate cancer patient usually has an elevated level of prostate-specific antigen (PSA) in blood, therefore, by quantitatively detecting the level of PSA in blood, early prostate cancer diagnostic can be achieved, which is of great importance to a successful subsequent treatment. In this section, several antigen-antibody reaction systems, in which both of the protein antigen and antibody are reviewed.

The sensor performance is reflected by the number of antigens that are captured by the immobilized antibodies through molecular recognition. Therefore, both the surface density and the molecular orientation of the immobilized antibodies determine the final antigen capture efficiency and the sensor performance. Figure 4 schematically shows an immunoglobulin G (IgG) molecule with four possible antibody orientations on a substrate surface. The antigen binding sites (fragment variable domain, Fv) are at the end of the two fragments antigen-bindings (Fabs). Ideally, the antibody should be immobilized with the fragment crystallisable region (Fc) standing on the substrate surface (end–on) to make the Fabs available for antigen capture. However, in reality, other orientations such as head-on (Fabs immobilized on the substrate surface), flat-on (both Fabs and Fc on the substrate surface) and side-on (one Fab and one Fc on the substrate surface) are also presented and the flat-on is the dominant one at the substrate surfaces (Xu et al. 2006; Xu et al. 2007; Zhao et al. 2011; Zhao et al. 2012b; Zhao et al. 2009). Therefore, a strategy which can stably immobilize an appropriate number of antibodies with the optimised molecular orientation on the sensor electrode surfaces, is crucial to ensure an effective analytical performance of an immunosensor. Different antibody immobilization strategies have been reported such as physical adsorption (Xu et al. 2006; Xu et al. 2007; Zhao et al. 2011; Zhao et al. 2012b; Zhao et al. 2009), covalent binding (Amiri et al. 2010; Chen et al. 2014; Corso et al. 2008; Hirlekar Schmid et al. 2006; Nimse and Kim 2013; Wu et al. 2006; Yang and Li 2005) and antibody-binding via proteins (Ikeda et al. 2009; Jeong et al. 2015; Zhao et al. 2012b). Table 2 briefly compares the advantages and disadvantages of these strategies. To maximise the potential of these strategies, combinations of each are increasingly applied to obtain an effective and efficient immobilization (Vashist et al. 2011).

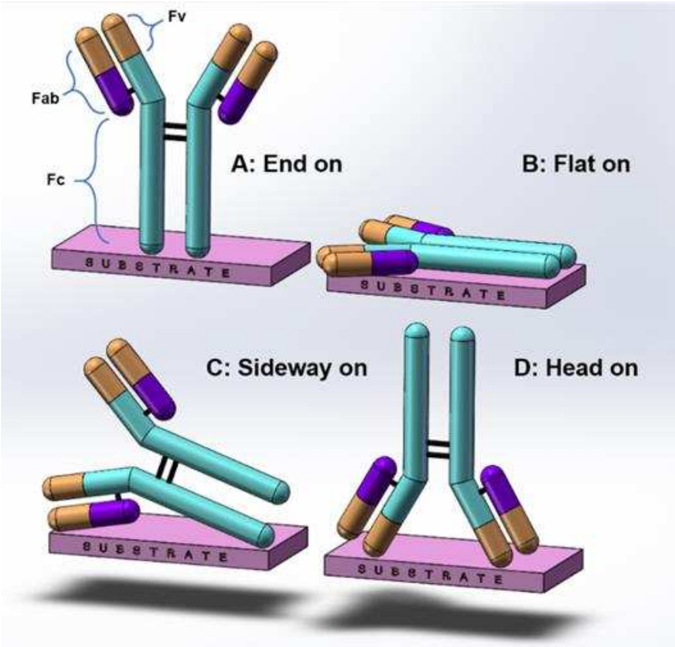

Figure 4. A schematic showing the possible orientations of an IgG molecule on a substrate surface. (Adapted from reference (Zhao et al. 2009))

Table 2. Comparison of common antibody immobilization strategies.

Strategy	Advantages	Disadvantages	Ref.
Physical adsorption	• Simple procedure • High antibody immobilization density	• Random orientation • Weak attachment • Denaturation of adsorbed antibodies	(Jung et al. 2008; Schramm et al. 1993)
Antibody-binding proteins (e.g. protein A, protein G)	• Controllable orientation • Immobilization at lower concentrations • High antigen binding efficiency	• Lower antibody immobilization density • Complicated and expensive procedure	(Peluso et al. 2003b; Schramm et al. 1993)
Covalent binding (e.g. NHS*, EDC*)	• Less denaturation • Stable immobilization • High antibody immobilization density	• Random orientation • Low antigen binding efficiency • Complicated procedure	(Danczyk et al. 2003; Jung et al. 2008)

*: NHS = N-hydroxysuccinimide; EDC = 1-ethyl-3-(3-dimethylaminopropyl)carbodiimide.

Real-time and label-free detection of PSA using FBARs have been investigated by different research groups in the last decade (Lin et al. 2011; Zhao et al. 2014; Zhao et al. 2011; Zhao et al. 2012b). The first prototype FBAR sensor which was able to detect PSA concentration in hundreds of ng/ml range was reported by Lin et al. (Lin et al. 2011) who immobilized the electrode surfaces with orientated antibodies (i.e. IgG) by using protein A as shown in Figure 5A. It has been reported that specifically orientated antibodies using protein A or G have increased binding activity compared to that of randomly immobilized antibodies (Ikeda et al. 2009; Jeong et al. 2015; Peluso et al. 2003a; Zhao et al. 2012b). For example, Jeong et al. (Jeong et al. 2015) have shown that antibodies immobilized on the protein-G-terminated glass slides significantly improved the orientation of antibodies for antigen binding and showed enhanced fluorescence intensity compared to that on the traditional epoxy-based slides (Figure 5B). When the antibody immobilized sensor was exposed to PSA, a clear f_r shift was observed, indicating a successful capture of PSA by immobilized antibodies. We have furthered this work by validating the results from FBAR frequency shift to the real mass change (Zhao et al. 2014). Mouse monoclonal antibody, anti-hPSA was immobilized onto the FBAR electrode surface to bind PSA. Parallel experiment was carried out by ellipsometry. By mapping the FBAR frequency shift with the data obtained from ellipsometry, the real mass change of the biomolecules on the gold electrode surfaces was obtained (Figure 6A). It was found that the optimum amount of antibody at the gold surface for effective antigen binding was around 1 mg/m^2 which can be achieved by adsorption for 15 min using an antibody solution at 5 mg/L or 2 min if using a 20 mg/L solution (Figure 6B). Subsequent bovine serum albumin (BSA) blocking was carried out to avoid the non-specific adsorption of antigens and resulted in a 70 kHz frequency downward shift. A further frequency downward shift of 46 kHz was observed by antigen binding and was found equivalent to 0.23 mg/m^2 antigen on the FBAR electrode surface. These results demonstrated that an FBAR can be used as a biosensor for quantitative detection of PSA level, and an increased PSA level indicates a potential of prostate cancer.

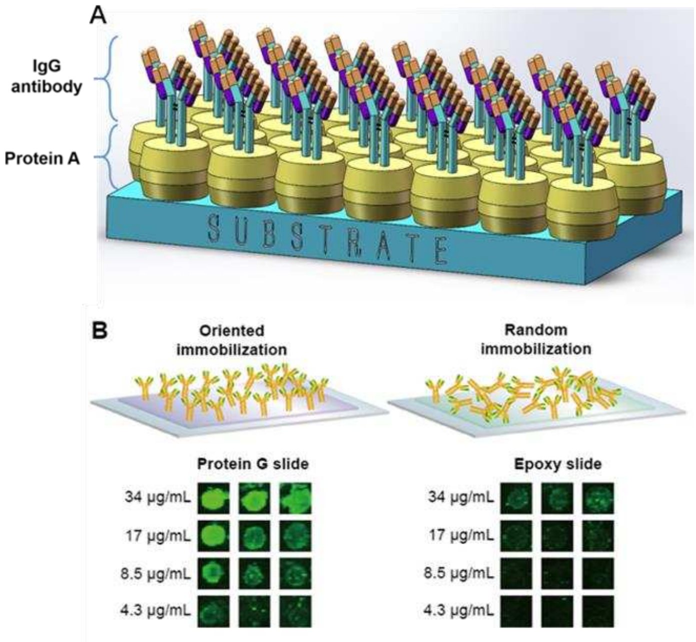

Figure 5. (A) Immobilization of antibodies on substrate using protein A. (Adapted from reference (Lin et al. 2011)) (B) Oriented immobilization of antibodies using protein G (left) and random immobilization (right). Representative images of the fluorescence intensity of human IgG bound to the capture antibodies immobilized on either protein G or epoxy-terminated glass slides with decreasing concentration of the antigen (34 – 4.3 µg/ml). (Adapted from reference (Jeong et al. 2015), © 2015 Jeong et al.)

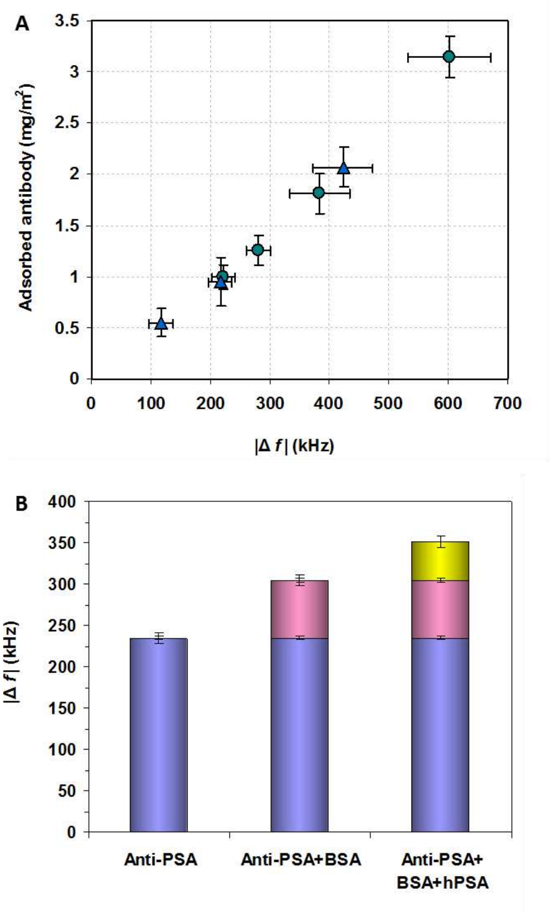

Figure 6. (A) Surface adsorbed amount of antibody obtained from ellipsometry plotted against FBAR frequency shift-down. (B) f_r shifts of FBAR after the adsorption of anti-hPSA antibody (5 mg/L) for 15 min, BSA (50 mg/L) blocking for 15 min and antigen (hPSA, 5 mg/L) binding for 15 min (Zhao et al. 2014). (Copyright © 2014 Elsevier Ltd.)

Other than PSA, FBARs have also been fabricated to detect other cancer biomarkers such as epithelial tumour marker (MUC1) (Guo et al. 2015; Zheng et al. 2016a), Alpha-fetoprotein (AFP) (Chen et al. 2011) and carcinoembryonic antigen (CEA) (Kim et al. 2013; Lee and Song 2010; Zheng et al. 2014; Zheng et al. 2016b). An AlN-based FBAR was fabricated with f_r approximately 575 MHz as an immunosensor to detect MUC1 (Guo et al. 2015). This sensor presented an expected linearity between the frequency shift and the concentrations of MUC1 (from 30 – 500 nM), and the sensitivity was then calculated to be 818.6 Hz/nM. Zheng et al. (Zheng et al. 2016a) reported that a ZnO-based FBAR achieved a higher sensitivity (4642.6 Hz/nM) and was used to detect MUC1, indicating the FBAR has a great potential to be used as an effective method to detect MUC1. Alpha-fetoprotein (AFP), another cancer marker, was also detected by using a ZnO-based FBAR with a f_r approximately 2.1 GHz (Chen et al. 2011). Because of this high operation frequency, the minimum detectable concentration of AFP was down to 1 ng/ml, indicating the FBAR can be a promising candidate for cancer diagnosis at a low analyte concentration.

Recently, FBAR has been extensively used to detect the carcinoembryonic antigen (CEA), a glycoprotein associated with breast, colorectal and lung cancer (Lee and Song 2010). Lee and Song used protein A and G to immobilize the anti-CEA for detection of CEA. It was found that the amount of anti-CEA captured by protein A and G increased with the concentration of the antibody used. Binding of antibody through protein A and G resulted in frequency shifts of 1810 and 2157 kHz respectively, when using 1 mg/ml antibody concentration. The subsequent CEA (1 mg/ml) capture resulted in frequency shifts of 370 and 659 kHz respectively. These results are highly consistent with the data obtained by Kim et al. (Kim et al. 2013) who used an AlN-based FBAR ($f_r \sim$ 2.5 GHz) to detect the CEA, beta actin, and BSA. Anti-CEA antibody was coated onto the electrode surface through protein A and protein G binding for the subsequent detection of CEA. It was found that the protein A method resulted in a 1893 kHz frequency shift for antibody immobilization and a 393 kHz for CEA binding, while the protein G method resulted in a 2173 kHz frequency shift for antibody immobilization and a 685 kHz frequency shift for CEA binding. The binding ratio for protein G is 10% higher than that of protein A (20.8%), indicating that protein G can immobilize more antibody than protein A and/or provide better antibody orientations. More recently, Zheng et al. (Zheng et al. 2014; Zheng et al. 2016b) have also used AlN-based FBARs to detect the CEA. Instead of anti-CEA antibody, the CEA binding aptamers were used as the biomarkers to capture the CEA molecules that were self-assembled on the top gold electrode. The aptamer modified FBAR was able to detect various concentrations of CEA ranging from 0.2 to 1 mg/ml. The frequency shift was found proportional to the mass loading. The presence of 0.2 mg/ml CEA resulted in a significant frequency shift of more than 1200 kHz compared to the negligible frequency shifts when the same concentration of carbohydrate antigen, beta actin, and BSA were used. The aptamer coated FBARs were found more effective in antigen-binding compared to anti-CEA coated FBARs. Meanwhile, it also has excellent specificity to the antigen.

FBAR has also been explored as an allergic sensing device. Immunoglobulins E (IgE) is one type of antibodies made by the immune system and associated with allergy. IgE attacks antigens, such as bacteria, viruses, and allergens. But overreactions of the human immune system can cause allergies. Chen et al. (Chen et al. 2015b) successfully detected human IgE by using a shear mode FBAR. More recently, DeMiguel-Ramos et al. (DeMiguel-Ramos et al. 2017) fabricated a shear mode FBAR with a sensitivity of 1800 kHz cm^2/pg to detect different concentrations of thrombin solutions by immobilizing a thrombin-binding aptamer on the electrode surface (Figure 7). The curves showed steeper slope with increasing concentration of the thrombin, demonstrated that the FBAR devices can not only measure the amount of thrombin binding, but also show the real time binding kinetics.

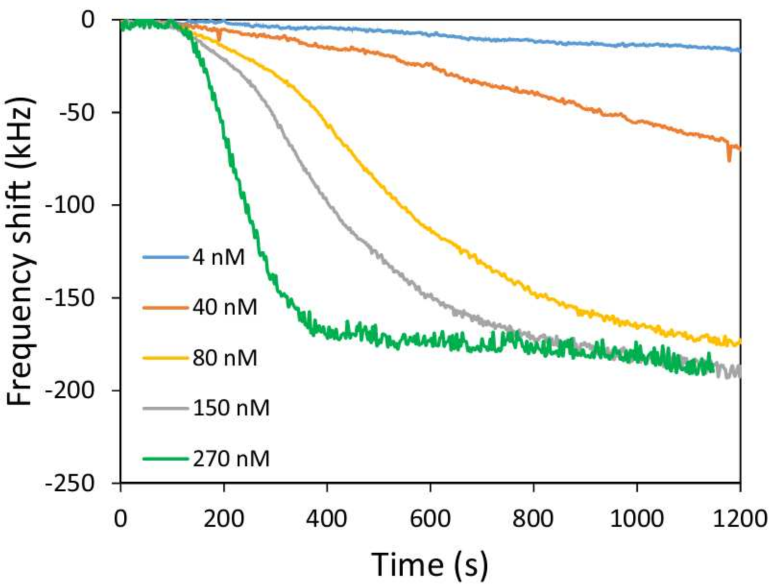

Figure 7. Shift of resonant frequency of FBAR sensors when exposed to thrombin solutions of different concentrations (4 - 270 nM). The saturation value is only achieved for concentrations of 80 nM and above (DeMiguel-Ramos et al. 2017). (Copyright © 2017 Elsevier Ltd.)

While the majority of FBAR biosensors are immunosensors, detecting antigens or antibodies as described above, a small amount of work has also been reported for detection of other protein using FBARs (Table 3). A high Q (130 in liquid) FBAR has been fabricated by Xu et al. (Xu et al. 2011) and was integrated with microfluidic channel for the detection of adsorption from three proteins with different molecular weights: albumin (67 kDa), IgG (150 kDa), and fibrinogen (340 kDa). The FBAR has a f_r of approximately 1.55 GHz and a mass sensitivity of 1358 Hz cm^2/ng. The three proteins with the same concentrations (0.1% w/v) were sequentially injected to the microfluidic channel with buffer wash between each sample (Figure 8A). The displacement of lower molecular weight protein by higher molecular weight proteins was clearly observed. The displacement of albumin by IgG resulted in a frequency downward shift of 700 kHz, equivalent to a 516 ng/cm^2 increased mass density, and the displacement of IgG by fibrinogen resulted in a frequency downward shift of 1100 kHz equivalent to a 810 ng/cm^2 increased mass density. This experiment demonstrated that the FBAR biosensor can effectively distinguish the adsorption of proteins with different molecular weights.

The frequency shift of FBAR has a good correlation with the protein concentration. Tukkiniemi et al. (Tukkiniemi et al. 2009) used the CMOS-integrated FBAR to detect the BSA adsorption from 0.001 to 1 mg/ml and found linear relationship between frequency shift and the protein concentration. This result is consistent with our previous work (García-Gancedo et al. 2011b). In addition, we found that the FBARs with carbon nanotubes (CNTs) top electrodes exhibited greater quality factors and increased gravimetric sensitivities. FBAR with CNTs as the top electrode exhibited a higher frequency change for a given load (~ 0.25 MHz cm^2/ng) compared to that with a metal electrode (~ 0.14 MHz cm^2/ng) (Figure 8B).

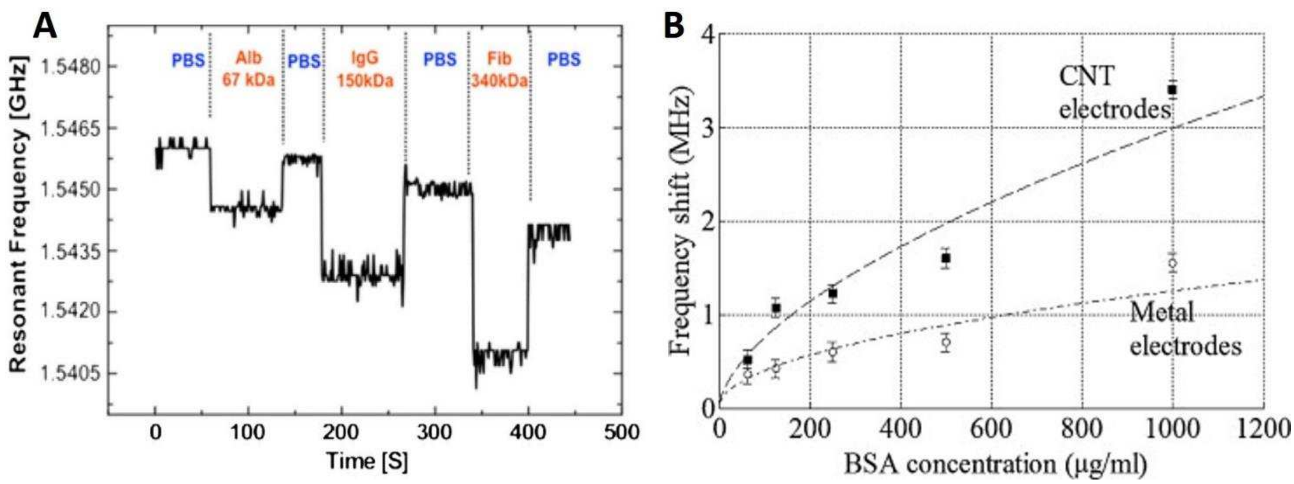

Figure 8. (A) Measured resonant frequency response of the FBAR sensors for the protein characterization of the Vroman effect. When a lower molecular weight protein adsorbed first to

the FBAR surface, and displaced by the higher molecular weight proteins (Alb→IgG→Fib). (Copyright © 2010 IEEE) (B) Frequency shift observed as a function of BSA concentration. The dashed lines are a guide for the eye. (Copyright © 2011 Elsevier Ltd.)

3.2. FBARs as DNA biosensors

In addition to proteins, FBARs have been increasingly applied to the detection of DNAs since 2004 (Gabl et al. 2004). There is an increasing need for the sensitive detection of DNA sequences for clinical diagnosis, environmental monitoring and food safety. For example, a real-time, label-free detection of DNA molecules or DNA hybridisation is of great interest for use in gene sequence analysis, which makes the detection of genetic mutation for early diseases diagnostic possible (Mastromatteo and Villa 2013). Gabl et al. (Gabl et al. 2004) reported that a label-free ZnO-based FBAR gravimetric biosensor was fabricated and successfully applied to the detection of DNA and protein molecules with a high operation frequency of 2 GHz. The sensitivity was then calculated to be 2400 Hz cm^2/ng which is approximately 2500 times higher than a QCM with a frequency of 20 MHz. Zhang et al. (Zhang et al. 2007) fabricated an Au top electrode FBAR to successfully detect DNA sequences (without labelling) by monitoring the f_r shifting when DNA hybridisation occurred. Figure 9A shows the schematic of the DNA sensor. The 15-mer probe nucleotide was functionalized at the 5'-end with a HS-$(CH_2)_6$- group for immobilization on the Au top electrode FBAR device. The unoccupied area was covered by mercapto-hexanol (MCH) to reduce the non-specific adsorption. The sensor was able to distinguish the sequences that have a single base mismatch to the probe sequences. Binding of complementary DNA resulted in a 70 kHz f_r shift while binding with one base mismatch DNA only resulted in a 25 kHz shift, demonstrated that the sensor is able to detect a single-nucleotide mismatch DNA sequence (Figure 9B). DNA detection process has also been performed in a diluted serum (1%) by using a shear mode FBAR (Auer et al. 2011). The minimum detectable concentration of DNA was down to 1 nM with a f_r of 800 MHz.

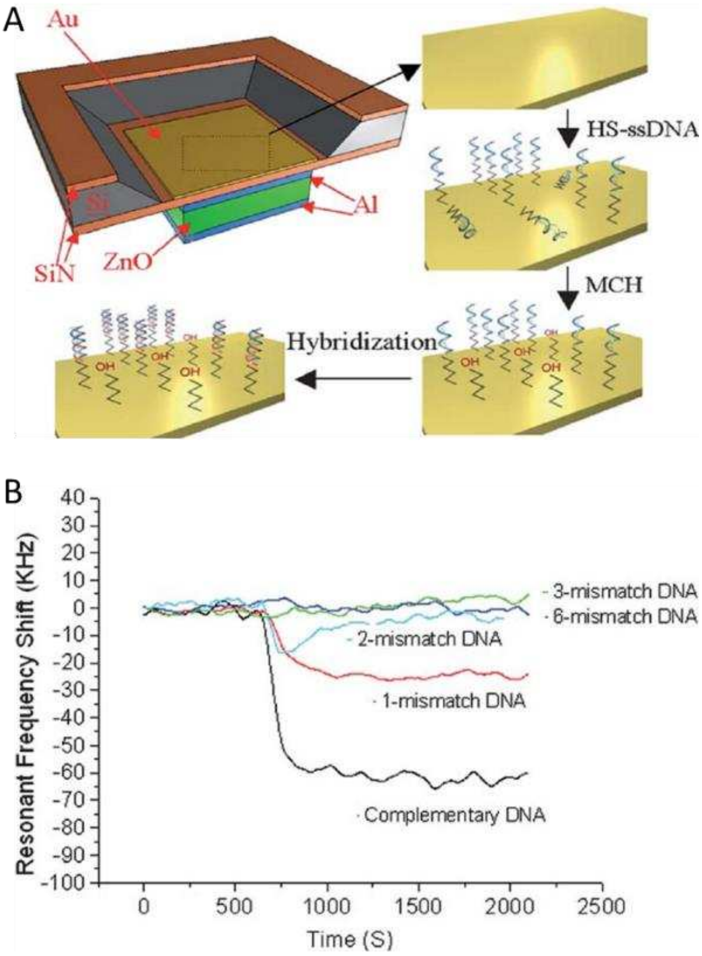

Figure 9. (A) Illustration of a FBAR device being treated with HS-ssDNA and MCH for mixed monolayer formation and then hybridized with a target DNA sequence. (B) The resonant frequency shift of the HS-DNA immobilized FBAR decreases when hybridized with the target DNA complements (Pang et al. 2012). (Copyright © 2012 The Royal Society of Chemistry)

3.3. FBARs as small ligands biosensors

FBARs have also been used as biosensors for the detection of small molecular ligands with very low molecular weights. For example, we have in the past used FBAR devices as odorant sensors (Zhao et al. 2012a). DEET (N,N-Diethyl-meta-toluamide, molecular weight 191 g/mol) is the most common active ingredient in insect repellents being highly effective against mosquitoes, and was therefore selected as a model molecular ligand (Bissinger et al. 2009; Paluch et al. 2010; Syed and Leal 2008). An odorant binding protein (AaegOBP22 originated from *Aedes aegypti* mosquitoes) was coated on a FBAR device as a biomarker for DEET. Alternate flow of the nitrogen gas with and without DEET vapour through the AaegOBP22 coated FBAR device resulted in a real-time frequency change of 8 – 10 kHz (Figure 10). This experiment demonstrated that FBAR devices are capable of detecting the DEET binding to the AaegOBP22 protein. As this is a reversible binding process, refreshing the sensor with nitrogen gas brought the f_r back to the baseline. This experiment also indicated that similar reversible binding processes can be potentially utilised by FBARs as electronic noses to efficiently detect specific bio-substances.

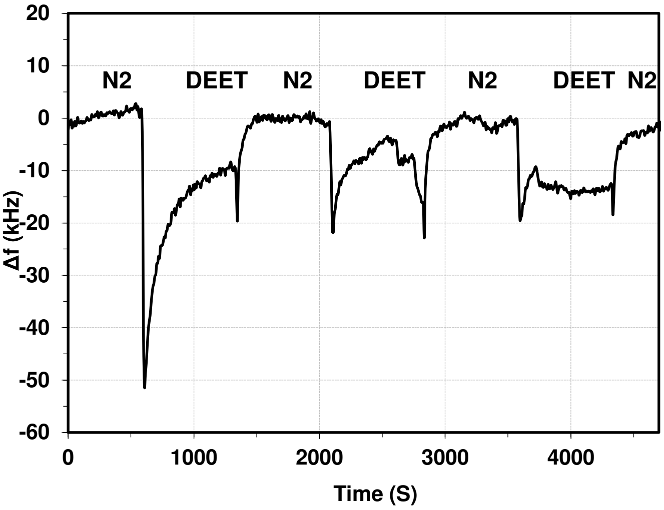

Figure 10. Responses of odorant binding protein coated FBAR sensors to N_2 gas with and without DEET vapour. Exposing the FBARs to DEET resulted in 8 – 10 kHz frequency drop (Zhao et al. 2012a). (Copyright © 2012 Elsevier Ltd.)

FBARs have also been used to detect small drug molecules such as cocaine (MW 303 g/mol) and heroin (MW 369 g/mol) (Wingqvist et al. 2007). Wingqvist et al. used a competitive binding method for their test. A synthetic antigen was first immobilized onto the FBAR electrode surface to capture the antibodies that can bind to both the synthetic antigen and the target analyte molecules. Introducing the analytes (Cocaine or Heroin) into the system resulted in a competitive binding and subsequent detachment of the captured antibodies, which resulted in an increase of the f_r. A concentration of 50 ng/ml heroin (a total amount of 2.5 ng binding on the electrode surface) resulted in a frequency change of 42 kHz compared to 10 – 15 Hz change from the QCM. This experiment demonstrated that FBAR devices are very sensitive to small amount of mass changes.

In the current context of anti-terrorism, it is of particular importance to develop highly sensitive and portable biosensors that can detect trace amount of explosive chemicals in public environment. FBARs have also been used for the detection of vapour traces of explosive chemicals such as TNT (Trinitrotoluene, M_W 227 g/mol) and RDX (Cyclotrimethylenetrinitramine, M_W 222 g/mol) (Lin et al. 2008a). Lin et al. functionalized the FBAR devices with antibodies through protein

A. The antibody functionalized FBAR devices were then used for the detection of TNT and RDX vapours. It was found that for the devices with a Q of 500 – 600 and f_r of 1.3 – 1.7 GHz, they have a detection threshold of 8 ppb (parts per billion) for TNT and 6 ppt (parts per trillion) for RDX, demonstrated a highly sensitive biosensor for public safety.

4. FBARs integrated with microfluidic devices

Since most of the biological applications are performed in liquid environments, it is essential that the FBAR sensors are able to work in liquids. FBARs are very small with typical cross-device size of less than 200 μm. Manual handling of liquids (bio-samples and reagents) for immobilization of biomarkers, reaction for bio-bonding, and buffer solution washing to remove non-specific bonding etc. is time consuming and costly with many potential mistakes. Hence, it is not practical to use standalone FBAR biosensors for the detection and diagnosis applications, but rather to integrate microfluidics to form lab-on-a-chip platforms for practical applications. Microfluidics can perform pumping and mixing of liquids containing biomarkers and bio-samples for immobilization, as well as bonding for continuous detection. Integration of FBARs with microfluidics has many advantages including fast operation, minimal use of bio-samples and reagents, no human-operation associated mistakes and cross contamination.

Currently, the major problem associated with applying acoustic wave-based biosensors for biological analysis in a liquid environment is the severe deterioration of performance of the biosensors due to the damping loss associated with liquid loading. The decrease in quality factor (Q) up to 90% was observed, which negatively affects the sensor's sensitivity (Zhang et al. 2009). In order to maintain FBARs with high Q, the key point is to reduce the acoustic energy loss caused by liquid loading. For FBARs operating in longitudinal mode, acoustic waves travel with displacement perpendicular to surface of the devices. Once used in a liquid environment, the acoustic energy will be dissipated by liquid and the FBARs will experience severe viscous damping, which results in great Q drops. (Enlund et al. 2010; Pang et al. 2012; Xu et al. 2011; Zhang et al. 2009). A reduction in Q of FBARs increases the noise floor in the f_r monitoring, hence the minimum detectable mass is increased. As mentioned in section 2.1, the thickness shear mode FBAR is better than the longitudinal mode one for the operation in liquids. Because a shear acoustic wave travels parallel to the surface of the device, there is no displacement perpendicular to the surface of the device, and therefore significantly less acoustic energy is lost and radiated into the liquid as compared to a longitudinal wave (Bjurström et al. 2006; Link et al. 2007; Pang et al. 2012; Weber et al. 2006). However, the wave velocity and f_r of a shear wave are typically lower than that of a longitudinal wave, and yet there are always some effects from the liquid loaded such as mass loading and small coupling of shear wave in liquid. As a result, the sensitivity of FBARs operated in the thickness shear mode is lower than that of FBARs operated in the longitudinal mode in dry condition. Nevertheless, for integration of FBARs with microfluidics, thickness shear mode FBARs have to be used.

Weber at al. (Weber et al. 2006) firstly reported the use of shear mode FBAR with a Bragg reflector to realize real-time monitoring of the binding process of antibody and antigen (i.e. anti-avidin/avidin) in a liquid environment. In order to compare the performance with those of QCM and longitudinal FBAR, both devices were adopted to conduct the measurement under similar conditions. The results showed that the shear mode FBAR had the best mass resolution (minimum detectable mass) which was 2.3 ng/cm^2 compared to 21 ng/cm^2 and 5.2 ng/cm^2 of the longitudinal mode FBAR and the QCM respectively, indicated shear mode FBARs are more suitable than longitudinal mode FABRs and QCMs for use in liquid environments as discussed above. There are a few reports on the integration of FBARs with microfluidics for detection. For example, Zheng at al. (Zheng et al. 2016b) integrated a shear mode AlN film-based FBAR with a microfluidic channel to detect CEA as mentioned above. Xu et al. (Xu et al. 2011) fabricated a lab-on-a-chip bio-detection system with the back-trench type FBAR biosensor being integrated inside the microfluidic channel. Polydimethylsiloxane (PDMS) was used to make microfluidic channels with transparent glass as the top cover of the channel. Furthermore, Xu et al. utilized the FBAR biosensor in Piers oscillator and built an electronic circuit to form a portable FBAR based bio-detection system. The most common proteins, albumin (Alb), IgG, and fibrinogen (Fib), in blood were used to study the competitive adsorption of proteins on the surface of the FBAR. The results showed that the FBAR-integrated microfluidic system can monitor the adsorption and reaction of proteins with high accuracy. Zhang et al. (Zhang et al. 2014a) successfully integrated an electrowetting-on-dielectric (EWOD) actuator with an AlN film-based FBAR on a single silicon chip/substrate, where the EWOD actuator manipulates digital droplets and the FBAR sensor detects analyte in the droplets. The merit of this integration is the sharing of AlN film between FBAR and EWOD actuator, which makes the integrated device compacter, capable of quantitative detection with many merits mentioned above. Figures 11A and 11B show the cross-section of integrated platform and the actual integrated device. A Hg^{2+} droplet of 10^{-7} M was then manipulated automatically by the EWOD and detected by the FBAR sensor (Figure 11C). A frequency downward shift of 28 kHz was successfully detected, which is not achievable if the FBAR is not integrated with a microfluidic device. More recently, Zheng at al. (Zheng et al. 2016b) also integrated a shear mode AlN film-based FBAR with a microfluidic channel to detect CEA. The frequency shift was found to be linearly correlated to the concentration (0.2 - 5 μg/L) of the anti-CEA aptamer used for coating the FBAR biosensor. Although the FBAR was not at high performance, the mass sensitivity was very high, approximately 2045 Hz cm^2/ng.

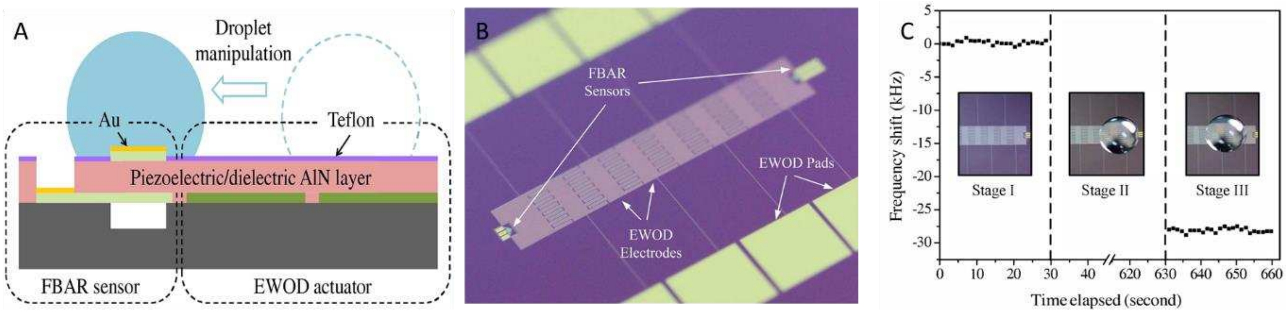

Figure 11. (A) A schematic cross-section of integrated device. Sample and reagent droplets are manipulated by the electrowetting-on-dielectric (EWOD) technology, and the FBAR sensor detects the presence of substances in the droplets. (B) Top view of the actual integrated device. Two FBAR sensors are placed at the two ends of the EWOD electrode array. (C) f_r tracking in Hg^{2+} detection experiment. In stage I, the FEAR sensor works in air; in stage II, an Hg^{2+} droplet of 10^{-7} M is loaded on the sensor by EWOD and the interaction between Au and Hg^{2+} and kept for 10 minutes; in stage III, the droplet is moved off the sensor by EWOD. A -28 kHz frequency shift is recorded. (Adapted from reference (Zhang et al. 2014a), Copyright © 2014 IEEE)

When integrating FBARs with microfluidic devices, the efficiency of mass transport becomes vital to obtain an accurate measurement. Wingqvist et al. (Wingqvist et al. 2007) studied the mass transport efficiency by conducting a comparison between a shear mode FBAR and a QCM. Figure 12 schematically shows a shear mode FBAR integrated with a microfluidic device. The statistic results indicated that the design of the microfluidic system was inefficient in terms of analyte utilization. A large portion of analyte was wasted instead of contributing to the detection process due to a low ratio of lateral dimension of FBAR (*L*) and the height of cavity (*H*) under the FBAR (i.e. *L/H* = 1). Therefore, this study demonstrated that the sensitivity can be optimised by a better design of microfluidic system.

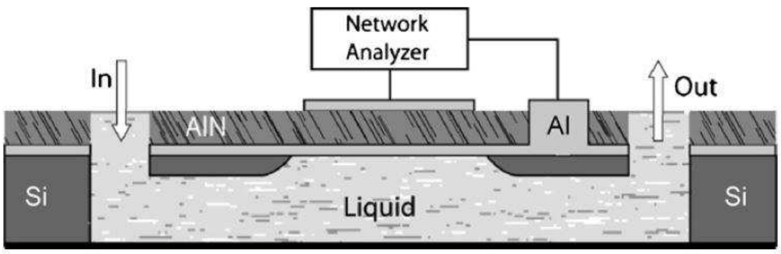

Figure 12. A schematic showing of a shear mode FBAR integrated with a microfluidic transport system (Wingqvist et al. 2007). (Copyright © 2007 Elsevier Ltd.)

Even though the integration of shear mode FBARs with microfluidic devices have been successful in accurately detecting analyte in liquid environments, the integrated systems can be further optimised in the following aspects: (1) choice of materials should efficiently wet the sensors' surface; (2) minimising the influence of the high frequency on the biochemistry; (3) suitable integration with the read-out electronics; (4) immobilization of biomarkers with optimal surface packing density and molecular orientation (Bange et al. 2005; Wingqvist et al. 2007).

5. FBAR arrays for high-throughput detection

As the size of FBARs can be fabricated as small as hundredths square micrometres, in addition to their flexible design and different shapes, it makes them possible for high-throughput detection using fabricated FBAR array. Tukkiniemi et al. (Tukkiniemi et al. 2009) pioneered the integration of FBARs with a CMOS read-out circuitry and used the integrated FBAR matrix sensors for the label-free detection of BSA. It was found that CMOS-integrated FBAR provided comparable noise and mass sensitivity compared to those using a network analyser. The mass resolution was measured to be 1 ng/cm^2 for both systems. Later, Nirschl et al. (Nirschl et al. 2010) fabricated an impedance-based CMOS with a 64 FBAR-array for the label-free detection of DNA and BSA. The integrated device has an effective test area smaller than 1 cm^2 (an area of a QCM crystal). Parallel experiments have been carried out to measure the adsorption on the electrode surface using FBAR, QCM and SPR. All three sensors showed the same trend with a very good correlation (Figure 13), and the mass sensitivity of the FBAR is nearly two orders of magnitude higher than the sensitivity of the QCM. Meanwhile, the CMOS integrated FBAR array can detect two different DNA sequences in a diluted human blood serum sample using pre-designed functionalisation. The label-free and real-time analysis capability of FBARs and their adaptability in array formats for simultaneous analysis of multiple targets make FBARs attractive candidates for high-throughput detection.

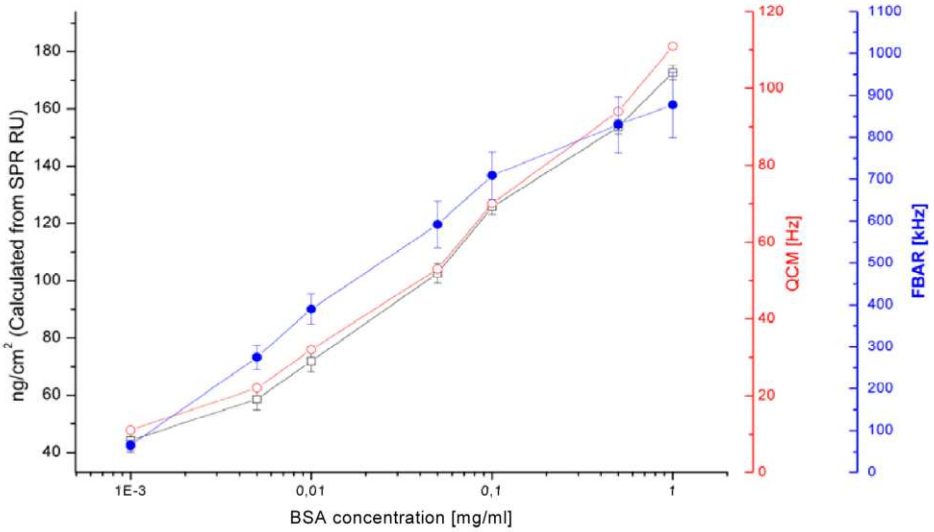

Figure 13. Titration curves for bovine serum albumin as measured with QCM (○), CMOS-integrated FBAR (●) and SPR (□). The curve for the FBAR measurement is the average of 10 pixels, the SPR represents 4 channels; the error bars show the standard deviation (Nirschl et al. 2010). (Copyright © Nirschl et al.)

The aforementioned examples illustrate that FBARs have been widely used in biological applications and achieved breakthrough successes. Table 3 summarises recent developments in FBAR as biosensors.

Table 3. Summary of recent developments using FBARs as biosensors.

Analyte	Piezoelectric material	Immobilized probes		Mass resolution / Sensitivity	Q	Frequency, f_r	LOD and/or linear range	Ref.
Proteins								
PSA	ZnO	IgG antibody	Immobilized by protein A	7.56 ng/cm^2	70	2.91 GHz	A few ng/ml	(Lin et al. 2011)
			Immobilized by protein G and DTSSP crosslinker	25 ng/cm^2		3.6 GHz		
	ZnO	Anti-hPSA, mouse monoclonal antibody		1.5 ng/cm^2	800	1.5 GHz	na	(Zhao et al. 2014)
CEA	AlN	Anti-CEA		3514 Hz cm^2/ng	na	2.477 GHz	0.2 – 0.8 mg/ml	(Lee and Song 2010)
	AlN	Aptamer		2045.89 Hz cm^2/ng	170	1.2 GHz	0.2 – 2.0 mg/ml	(Zheng et al. 2016b)
	AlN	Aptamer		2284 Hz cm^2/ng	520	1997.05 MHz	0.2 – 1.0 mg/ml	(Zheng et al. 2014)
AFP	ZnO	Anti-AFP		48 kHz cm^2/ng	na	2.1 GHz	1 ng/ml	(Chen et al. 2011)
IgE	AlN	Anti-Human IgE		1.425×10^5 cm^2/g (7.0 μg/cm^2)	na	1.175 GHz	na	(Chen et al. 2015b)
MUC1	AlN	Streptavidin and AuNPs-MUC1 aptamers		818.6 Hz/nM	384	575 MHz	30 – 500 nM	(Guo et al. 2015)
	ZnO	Streptavidin and AuNPs-MUC1 aptamers		4642.6 Hz/nM	224	1503.3 MHz	20 – 500 nM	(Zheng et al. 2016a)
Anti-avidin	ZnO	Avidin		585 Hz cm^2/ng	100 – 150	790 MHz	2.3 ng/cm^2	(Weber et al. 2006)
Thrombin / IgG	AlN	Thrombin-binding aptamer IgG antibody		1800 kHz cm^2/pg	na	1.3 GHz	4 nM	(DeMiguel-Ramos et al. 2017)
Alb/ IgG/	ZnO	/		1358 Hz cm^2/ng	130-150	1.55 GHz	1.35 ng/cm^2	(Xu et al. 2011)

Fibrinogen							
BSA	ZnO	/	1 ng/cm^2	150	~800 MHz	na	(Tukkiniemi et al. 2009)
BSA	AlN	/	0.25 MHz cm^2/ng	> 2000	1.75 GHz	na	(García-Gancedo et al. 2011b)
DNA							
ssDNA	ZnO	Disulphide-modified ssDNA probes	1 ng/cm^2	na	800 MHz	1 nM	(Auer et al. 2011)
DNA synthesis	ZnO	Thiol-modified DNA primer	105 ng/cm^2	32	3.16 GHz	na	(Lin et al. 2010)
ssDNA	ZnO	Thiol-modified 25 bases ssDNA probe	2 kHz cm^2/ng	na	800 MHz	1 ng/cm^2	(Nirschl et al. 2010)
Mismatching DNA sequences	ZnO	Thiol-modified 15 bases ssDNA probe	na	na	1 GHz	na	(Zhang et al. 2007)
ssDNA	ZnO	Thiol-modified 25 bases ssDNA probe	2400 Hz cm^2/ng	330	2 GHz	na	(Gabl et al. 2004)
Small Ligands							
DEET	ZnO	Binding protein (AaegOBP22)	0.2 MHz cm^2/ng	800	~1.5 GHz	na	(Zhao et al. 2012a)
Parathion/antibody	AlN	Artificial antigens	2.23 $/_{50}$(μg/L)	386	2 GHz	0.08 μg/L	(Wang et al. 2014a)
Chlorpyrifos	ZnO	Acetylcholinesterase (AChE) enzyme	17$/_{50}$(μg/L)	298	1.47 GHz	4.1×10^{-2} nM	(Chen et al. 2012)
Cocaine Heroin	AlN	Antibodies with specificity towards both the coated synthetic antigen and target molecules	54 kHz μL/ng 84 kHz μL/ng	na	800 MHz	na	(Wingqvist et al. 2007)
TNT XRD	ZnO	Antibody	0.96 ppm/ppb 10.4 ppm/ppb	500 – 600	1.96 GHz 1.65 GHz	na na	(Lin et al. 2008a)

6. Conclusions and Future perspectives

FBARs have many advantages over their counterparts such as high sensitivity, easy operation, small size and low cost, all of which make them increasingly popular for a wide range of applications such as immunoassays, the detection of DNA mutation and other small molecules. This review presents the recent developments of FBARs in the following aspects: (1) materials used for fabricating FBARs; (2) the optimisation methods for improving the detection performances of FBARs and; (3) the biological applications of FBARs as biosensors. Since the quality of the piezoelectric thin films is of great importance to fabricate a high performance FBAR, a film with a highly organized microstructure, good piezoelectric properties, high k^2 is desired. ZnO and AlN are the most optimising piezoelectric materials used for fabrication of FBARs not only because of their good inherent physical properties which mentioned above, but also owing to their simple fabrication processes and low cost. In order to further improve the performances of FBARs, several methods have been used to optimise the sensitivity of FBARs, such as CNT coated electrodes and varying the shape of electrodes. In terms of biological applications, the shear mode FBARs are promising candidates owing to their excellent capability of maintaining high Q value during their operation in liquid environments, hence the shear mode FBARs have been widely used to detect proteins, DNA, and small ligands. For the detection of proteins, FBARs have been mainly used as immunosensors which are based on antibody-antigen interactions. PSA, MUC1, AFP, CEA and IgE have been successfully detected by using FBARs. In addition to proteins, FBARs have been increasingly used to detect DNA for the analysis of DNA sequences which is essential to the determination of genetic mutation. Small ligands such as DEET, cocaine, heroin and TNT in very low concentrations have also been successfully detected by using FBARs, indicating that FBARs are very sensitive to small amount of mass changes. FBARs are also integrated with microfluidic devices to improve their sensing speed and accuracy, which is a critical step for fabricating lab-on-a-chip diagnostic systems. Additionally, the small size and flexible design of FBARs are advantageous as their arrays have been used for high-throughput detection of multiple targets with significant success.

Although FBARs have gained breakthrough success in a variety of biological applications, they can be further optimised to improve their detection performances in the following aspects but not limited to: (1) choice of media materials integrated with FBARs should generate higher frequency, hence higher sensitivity; (2) materials used in shear mode FBARs should efficiently wet the sensors' surface; (3) minimising the influence of the high frequency on the biochemistry to reduce the potential side effects; (4) integration with suitable read-out electronics and other sensing technologies to achieve multifunctional sensors with high sensitivity; (5) immobilization of biomarkers with optimal surface packing density and molecular orientation on sensor electrodes to improve the efficiency of analyte detection (Bange et al. 2005; Wingqvist et al. 2007).

References

Akiyama, M., Kamohara, T., Kano, K., Teshigahara, A., Takeuchi, Y., Kawahara, N., 2009. Enhancement of piezoelectric response in scandium aluminum nitride alloy thin films prepared by dual reactive cosputtering. Advanced Materials 21(5), 593-596.

Amiri, A., Choi, E.Y., Kim, H.J., 2010. Development and molecular recognition of Calixcrownchip as an electrochemical ALT immunosensor. Journal of Inclusion Phenomena and Macrocyclic Chemistry 66(1-2), 185-194.

Arce, L., Zougagh, M., Arce, C., Moreno, A., Rios, A., Valcárcel, M., 2007. Self-assembled monolayer-based piezoelectric flow immunosensor for the determination of canine immunoglobulin. Biosensors and Bioelectronics 22(12), 3217-3223.

Auer, S., Nirschl, M., Schreiter, M., Vikholm-Lundin, I., 2011. Detection of DNA hybridisation in a diluted serum matrix by surface plasmon resonance and film bulk acoustic resonators. Analytical and Bioanalytical Chemistry 400(5), 1387-1396.

Ayala, V., Moosmann, K., Prucker, O., Rühe, J., Reindl, L., 2009. Chemical Modification of Surfaces for Biochemical and Medical Sensor Applications. World Congress on Medical Physics and Biomedical Engineering, September 7-12, 2009, Munich, Germany, pp. 339-342. Springer.

Bange, A., Halsall, H.B., Heineman, W.R., 2005. Microfluidic immunosensor systems. Biosensors and Bioelectronics 20(12), 2488-2503.

Bian, X., Jin, H., Wang, X., Dong, S., Chen, G., Luo, J.K., Deen, M.J., Qi, B., 2015. UV sensing using film bulk acoustic resonators based on Au/n-ZnO/piezoelectric-ZnO/Al structure. Sci Rep 5, 9123.

Bissinger, B., Apperson, C., Sonenshine, D., Watson, D., Roe, R., 2009. Efficacy of the new repellent BioUD® against three species of ixodid ticks. Experimental and Applied Acarology 48(3), 239-250.

Bjurstrom, J., Wingqvist, G., Katardjiev, I., 2006. Synthesis of textured thin piezoelectric AlN films with a nonzero C-axis mean tilt for the fabrication of shear mode resonators. IEEE Transactions on Ultrasonics, Ferroelectrics and Frequency Control 53(11), 2095-2100.

Bjurström, J., Wingqvist, G., Yantchev, V., Katardjiev, I., 2006. Design and fabrication of temperature compensated liquid FBAR sensors. IEEE Int. Ultrasonic Symposium, 3-6 October, Vancouver, Canada.

Cao, C., Kim, J.P., Kim, B.W., Chae, H., Yoon, H.C., Yang, S.S., Sim, S.J., 2006. A strategy for sensitivity and specificity enhancements in prostate specific antigen-α 1-antichymotrypsin detection based on surface plasmon resonance. Biosensors and Bioelectronics 21(11), 2106-2113.

Caruso, F., Rodda, E., Furlong, D.N., Niikura, K., Okahata, Y., 1997. Quartz crystal microbalance study of DNA immobilization and hybridization for nucleic acid sensor development. Analytical Chemistry 69(11), 2043-2049.

Chang, Y., Tang, N., Qu, H., Liu, J., Zhang, D., Zhang, H., Pang, W., Duan, X., 2016. Detection of Volatile Organic Compounds by Self-assembled Monolayer Coated Sensor Array with Concentration-independent Fingerprints. Sci Rep 6, 23970.

Chen, D., Wang, J., Xu, Y., Li, D., 2012. A pure shear mode ZnO film resonator for the detection of organophosphorous pesticides. Sensors and Actuators B: Chemical 171-172, 1081-1086.

Chen, D., Wang, J.J., Li, D.H., Li, Z.X., 2011. Film bulk acoustic resonator based biosensor for detection of cancer serological marker. Electronics Letters 47(21), 1169.

Chen, G., Zhao, X., Wang, X., Jin, H., Li, S., Dong, S., Flewitt, A., Milne, W., Luo, J., 2015a. Film bulk acoustic resonators integrated on arbitrary substrates using a polymer support layer. Scientific reports 5.

Chen, H., Liu, F., Qi, F., Koh, K., Wang, K., 2014. Fabrication of calix [4] arene derivative monolayers to control orientation of antibody immobilization. International journal of molecular sciences 15(4), 5496-5507.

Chen, Q., Wang, Q.M., 2005. The effective electromechanical coupling coefficient of piezoelectric thin-film resonators. Applied Physics Letters 86(2), 022904.

Chen, Y.C., Shih, W.C., Chang, W.T., Yang, C.H., Kao, K.S., Cheng, C.C., 2015b. Biosensor for human IgE detection using shear-mode FBAR devices. Nanoscale Res Lett 10, 69.

Choi, N.K., Kim, K.B., Kim, Y.I., Kim, M.S., 2014. Effect of design parameters on thin film bulk acoustic resonator performance. Journal of Electroceramics 33(1-2), 17-24.

Corso, C.D., Dickherber, A., Hunt, W.D., 2008. An investigation of antibody immobilization methods employing organosilanes on planar ZnO surfaces for biosensor applications. Biosens Bioelectron 24(4), 811-817.

Corso, C.D., Stubbs, D.D., Lee, S.H., Goggins, M., Hruban, R.H., Hunt, W.D., 2006. Real-time detection of mesothelin in pancreatic cancer cell line supernatant using an acoustic wave immunosensor. Cancer Detect Prev 30(2), 180-187.

Danczyk, R., Krieder, B., North, A., Webster, T., HogenEsch, H., Rundell, A., 2003. Comparison of antibody functionality using different immobilization methods. Biotechnology and bioengineering 84(2), 215-223.

DeMiguel-Ramos, M., Díaz-Durán, B., Escolano, J.-M., Barba, M., Mirea, T., Olivares, J., Clement, M., Iborra, E., 2017. Gravimetric biosensor based on a 1.3 GHz AlN shear-mode solidly mounted resonator. Sensors and Actuators B: Chemical 239, 1282-1288.

DeMiguel-Ramos, M., Olivares, J., Clement, M., Mirea, T., Sangrador, J., Iborra, E., Barba, M., 2014. AlN shear mode solidly mounted resonator with temperature compensation for in-liquid sensing. SENSORS, 2014 IEEE, pp. 966-969. IEEE.

Dickherber, A., Corso, C.D., Hunt, W.D., 2008. Optimization and characterization of a ZnO biosensor array. Sensors and Actuators A: Physical 144(1), 7-12.

Dragoman, M., Muller, A., Neculoiu, D., Vasilache, D., Konstantinidis, G., Grenier, K., Dubuc, D., Bary, L., Plana, R., Flahaut, E., 2006. High performance thin film bulk acoustic resonator covered with carbon nanotubes. Applied physics letters 89(14), 143122.

Enlund, J., Martin, D.M., Yantchev, V., Katardjiev, I., 2010. FBAR Sensor Array for in Liquid Operation. IEEE Sensors Journal 10(12), 1903-1904.

Esconjauregui, S., Makaryan, T., Mirea, T., DeMiguel-Ramos, M., Olivares, J., Guo, Y., Sugime, H., D'Arsié, L., Yang, J., Bhardwaj, S., Cepek, C., Robertson, J., Iborra, E., 2015. Carbon nanotube forests as top electrode in electroacoustic resonators. Applied Physics Letters 107(13), 133106.

Fanget, S., Hentz, S., Puget, P., Arcamone, J., Matheron, M., Colinet, E., Andreucci, P., Duraffourg, L., Myers, E., Roukes, M., 2011. Gas sensors based on gravimetric detection—A review. Sensors and Actuators B: Chemical 160(1), 804-821.

Flewitt, A., Luo, J., Fu, Y.Q., Garcia-Gancedo, L., Du, X., Lu, J., Zhao, X., Iborra, E., Ramos, M., Milne, W., 2015. ZnO based SAW and FBAR devices for bio-sensing applications. Journal of Non-Newtonian Fluid Mechanics 222, 209-216.

Fu, Y.Q., Luo, J., Du, X., Flewitt, A., Li, Y., Markx, G., Walton, A., Milne, W., 2010. Recent developments on ZnO films for acoustic wave based bio-sensing and microfluidic applications: a review. Sensors and Actuators B: Chemical 143(2), 606-619.

Fu, Y.Q., Luo, J., Nguyen, N.T., Walton, A., Flewitt, A., Zu, X.T., Li, Y., McHale, G., Matthews, A., Iborra, E., 2017. Advances in piezoelectric thin films for acoustic biosensors, acoustofluidics and lab-on-chip applications. Progress in Materials Science.

Gabl, R., Feucht, H.D., Zeininger, H., Eckstein, G., Schreiter, M., Primig, R., Pitzer, D., Wersing, W., 2004. First results on label-free detection of DNA and protein molecules using a novel integrated sensor technology based on gravimetric detection principles. Biosensors and Bioelectronics 19(6), 615-620.

Gao, J., Liu, G., Li, J., Li, G., 2016. Recent developments of film bulk acoustic resonators. Functional Materials Letters 09(03), 1630002.

Garcia-Gancedo, L., Al-Naimi, F., Flewitt, A., Milne, W., Ashley, G., Luo, J., Zhao, X., Lu, J., 2010a. Fabrication of high-Q film bulk acoustic resonator (FBAR) filters with carbon nanotube (CNT) electrodes. Ultrasonics Symposium (IUS), 2010 IEEE, pp. 301-304. IEEE.

Garcia-Gancedo, L., Al-Naimi, F., Flewitt, A.J., Milne, W.I., Ashley, G.M., Luo, J.K., Zhao, X., Lu, J.R., 2011a. ZnO-based FBAR resonators with carbon nanotube electrodes. IEEE Transactions on Ultrasonics Ferroelectrics and Frequency Control 58(11), 2438.

Garcia-Gancedo, L., Pedrós, J., Flewitt, A.J., Milne, W.I., Ashley, G.M., Luo, J., Ford, C.J., 2010b. Ultrafast sputtered ZnO thin films with high k T for acoustic wave device applications. Ultrasonics Symposium (IUS), 2010 IEEE, pp. 1064-1067. IEEE.

García-Gancedo, L., Pedrós, J., Iborra, E., Clement, M., Zhao, X., Olivares, J., Capilla, J., Luo, J., Lu, J., Milne, W., 2013. Direct comparison of the gravimetric responsivities of ZnO-based FBARs and SMRs. Sensors and Actuators B: Chemical 183, 136-143.

García-Gancedo, L., Zhu, Z., Iborra, E., Clement, M., Olivares, J., Flewitt, A., Milne, W., Ashley, G., Luo, J., Zhao, X., 2011b. AlN-based BAW resonators with CNT electrodes for gravimetric biosensing. Sensors and Actuators B: Chemical 160(1), 1386-1393.

Ge, Z., Lin, M., Wang, P., Pei, H., Yan, J., Shi, J., Huang, Q., He, D., Fan, C., Zuo, X., 2014. Hybridization chain reaction amplification of microRNA detection with a tetrahedral DNA nanostructure-based electrochemical biosensor. Analytical chemistry 86(4), 2124-2130.

Giangu, I., Stavrinidis, G., Stefanescu, A., Stavrinidis, A., Dinescu, A., Konstantinidis, G., Müller, A., 2015. Pressure sensors based on high frequency operating GaN FBARs. Semiconductor Conference (CAS), 2015 International, pp. 99-102. IEEE.

Gu, C., Xuan, W., Dong, S., Wang, X., Li, H., Yu, L., Luo, J., 2018. Temperature calibrated on-chip dual-mode film bulk acoustic resonator pressure sensor with a sealed back-trench cavity. Journal of Micromechanics and Microengineering 28(7), 075010.

Guo, P., Xiong, J., Zheng, D., Zhang, W., Liu, L., Wang, S., Gu, H., 2015. A biosensor based on a film bulk acoustic resonator and biotin–avidin system for the detection of the epithelial tumor marker mucin 1. RSC Adv. 5(81), 66355-66359.

Hansen, K.M., Thundat, T., 2005. Microcantilever biosensors. Methods 37(1), 57-64.

He, X.F., Liu, X., Yin, X.F., Wen, Z.Y., Chen, K.W., 2011. Active control scheme for improving mass resolution of film bulk acoustic resonators. Applied Mathematics and Mechanics 32(6), 749-756.

Hirlekar Schmid, A., Stanca, S.E., Thakur, M.S., Thampi, K.R., Raman Suri, C., 2006. Site-directed antibody immobilization on gold substrate for surface plasmon resonance sensors. Sensors and Actuators B: Chemical 113(1), 297-303.

Hirsh, R., 2006. Non-invasive method and device to monitor cardiac parameters. Google Patents.

Hu, Y., Zuo, P., Ye, B.-C., 2013. Label-free electrochemical impedance spectroscopy biosensor for direct detection of cancer cells based on the interaction between carbohydrate and lectin. Biosensors and Bioelectronics 43, 79-83.

Ikeda, T., Hata, Y., Ninomiya, K., Ikura, Y., Takeguchi, K., Aoyagi, S., Hirota, R., Kuroda, A., 2009. Oriented immobilization of antibodies on a silicon wafer using Si-tagged protein A. Anal Biochem 385(1), 132-137.

Islam, M.S., Kouzani, A.Z., Dai, X.J., Michalski, W.P., 2011. Investigation of the effects of design parameters on sensitivity of surface plasmon resonance biosensors. Biomedical Signal Processing and Control 6(2), 147-156.

Jeong, Y., Lee, K.H., Park, H., Choi, J., 2015. Enhanced detection of single-cell-secreted proteins using a fluorescent immunoassay on the protein-G-terminated glass substrate. International journal of nanomedicine 10, 7197.

Jun Phil, J., Jin Bock, L., Myung Ho, L., Jin Seok, P., 2003. Experimental and theoretical investigation on the relationship between AlN properties and AlN-based FBAR characteristics. IEEE International Frequency Control Symposium and PDA Exhibition Jointly with the 17th European Frequency and Time Forum, 2003. Proceedings of the 2003, pp. 779-784.

Jung, Y., Jeong, J.Y., Chung, B.H., 2008. Recent advances in immobilization methods of antibodies on solid supports. Analyst 133(6), 697-701.

Kanazawa, K.K., 1997. Mechanical behaviour of films on the quartz microbalance. Faraday Discussions 107, 77-90.

Kang, D.J., Kim, J.S., Jeong, S.W., Roh, Y., Jeong, S.H., Boo, J.H., 2005. Structural and electrical characteristics of R.F. magnetron sputtered ZnO films. Thin Solid Films 475(1), 160-165.

Kanno, S., Yanagida, Y., Haruyama, T., Kobatake, E., Aizawa, M., 2000. Assembling of engineered IgG-binding protein on gold surface for highly oriented antibody immobilization. Journal of biotechnology 76(2), 207-214.

Katardjiev, I., Yantchev, V., 2012. Recent developments in thin film electro-acoustic technology for biosensor applications. Vacuum 86(5), 520-531.

Khanna, A., Gane, E., Chong, T., 2003. A 2GHz voltage tunable FBAR oscillator. Microwave Symposium Digest, 2003 IEEE MTT-S International, pp. 717-720. IEEE.

Kim, E., Choi, Y.K., Song, J., Lee, J., 2013. Detection of various self-assembled monolayers by AlN-based film bulk acoustic resonator. Materials Research Bulletin 48(12), 5076-5079.

Kim, H.J., Kim, Y.B., Park, J., Kim, T.S., 2003. Biological element detection sensor application of micromachined PZT thick film cantilever. Sensors, 2003. Proceedings of IEEE, pp. 1054-1058. IEEE.

Kim, H.Y., Kim, K.B., Cho, S.H., Kim, Y.I., 2012. Analysis of resonance characteristics of Bragg reflector type film bulk acoustic resonator. Surface and Coatings Technology 211, 143-147.

Koohi, M.Z., Mortazawi, A., 2017. BST thin film bulk acoustic resonator optimization for un-cooled IR sensors application. European Microwave Conference (EuMC), 2017 47th, pp. 328-330. IEEE.

Kößlinger, C., Drost, S., Aberl, F., Wolf, H., Koch, S., Woias, P., 1992. A quartz crystal biosensor for measurement in liquids. Biosensors and Bioelectronics 7(6), 397-404.

Krishnaswamy, S., Rosenbaum, J., Horwitz, S., Vale, C., Moore, R., 1990. Film bulk acoustic wave resonator technology. Ultrasonics Symposium, 1990. Proceedings., IEEE 1990, pp. 529-536. IEEE.

Lee, J.B., Kim, H.J., Kim, S.G., Hwang, C.S., Hong, S.-H., Shin, Y.H., Lee, N.H., 2003. Deposition of ZnO thin films by magnetron sputtering for a film bulk acoustic resonator. Thin Solid Films 435(1), 179-185.

Lee, S., Kim, K.B., Kim, Y.I., 2011. Love wave SAW biosensors for detection of antigen-antibody binding and comparison with SPR biosensor. Food Science and Biotechnology 20(5), 1413.

Lee, S.H., Jung, Y., Kim, T., Kim, T., Kim, Y., Jung, S., 2015. Polymer coated film bulk acoustic resonator (FBAR) arrays for Indoor Air Quality (IAQ) monitoring. SENSORS, 2015 IEEE, pp. 1-4. IEEE.

Lee, T.Y., Song, J.T., 2010. Detection of carcinoembryonic antigen using AlN FBAR. Thin Solid Films 518(22), 6630-6633.

Lee, Y., Lim, G., Moon, W., 2007. A piezoelectric micro-cantilever bio-sensor using the mass-micro-balancing technique with self-excitation. Microsystem Technologies 13(5-6), 563-567.

Liedberg, B., Nylander, C., Lunström, I., 1983. Surface plasmon resonance for gas detection and biosensing. Sensors and actuators 4, 299-304.

Lin, A., Li, Y.J., Wang, L., Chen, S.J., Gross, M.E., Kim, E.S., 2011. Label-free detection of prostate-specific antigen with FBAR-based sensor with oriented antibody immobilization. Ultrasonics Symposium (IUS), 2011 IEEE International, pp. 797-800. IEEE.

Lin, A., Sahin, F.E., Chen, S.-J., Pham, P., Kim, E.S., 2010. Real-time label-free detection of DNA synthesis by FBAR-based mass sensing. Ultrasonics Symposium (IUS), 2010 IEEE, pp. 1286-1289. IEEE.

Lin, A., Yu, H., Waters, M.S., Kim, E.S., Goodman, S.D., 2008a. Explosive trace detection with FBAR-based sensor. Micro Electro Mechanical Systems, 2008. MEMS 2008. IEEE 21st International Conference on, pp. 208-211. IEEE.

Lin, R.C., Chen, Y.C., Chang, W.T., Cheng, C.C., Kao, K.S., 2008b. Highly sensitive mass sensor using film bulk acoustic resonator. Sensors and Actuators A: Physical 147(2), 425-429.

Lin, Y.C., Hong, C.R., Chuang, H.A., 2008c. Fabrication and analysis of ZnO thin film bulk acoustic resonators. Applied Surface Science 254(13), 3780-3786.

Link, M., Weber, J., Schreiter, M., Wersing, W., Elmazria, O., Alnot, P., 2007. Sensing characteristics of high-frequency shear mode resonators in glycerol solutions☆. Sensors and Actuators B: Chemical 121(2), 372-378.

Liu, B., Chen, X., Cai, H., Mohammad Ali, M., Tian, X., Tao, L., Yang, Y., Ren, T., 2016. Surface acoustic wave devices for sensor applications. Journal of Semiconductors 37(2), 021001.

Liu, Q., Flewitt, A.J., 2014. On-chip temperature-compensated love mode surface acoustic wave device for gravimetric sensing. Applied Physics Letters 105(21), 213511.

Liu, W., Wang, J., Yu, Y., Chang, Y., Tang, N., Qu, H., Wang, Y., Pang, W., Zhang, H., Zhang, D., Xu, H., Duan, X., 2015. Tuning the resonant frequency of resonators using molecular surface self-assembly approach. ACS Appl Mater Interfaces 7(1), 950-958.

Lu, Y., Chang, Y., Tang, N., Qu, H., Liu, J., Pang, W., Zhang, H., Zhang, D., Duan, X., 2015. Detection of Volatile Organic Compounds Using Microfabricated Resonator Array Functionalized with Supramolecular Monolayers. ACS Appl Mater Interfaces 7(32), 17893-17903.

Mai, L., Kim, D.-H., Yim, M., Yoon, G., 2004. A feasibility study of ZnO-based FBAR devices for an ultra-mass-sensitive sensor application. Microwave and Optical Technology Letters 42(6), 505-507.

Manickam, A., Johnson, C.A., Kavusi, S., Hassibi, A., 2012. Interface Design for CMOS-Integrated Electrochemical Impedance Spectroscopy (EIS) Biosensors. Sensors 12(11), 14467.

Marx, K.A., 2003. Quartz crystal microbalance: a useful tool for studying thin polymer films and complex biomolecular systems at the solution− surface interface. Biomacromolecules 4(5), 1099-1120.

Mastromatteo, U., Villa, F.F., 2013. High sensitivity acoustic wave AlN/Si mass detectors arrays for artificial olfactory and biosensing applications: A review. Sensors and Actuators B: Chemical 179, 319-327.

Montagut, Y., Narbon, J.G., Jiménez, Y., March, C., Montoya, Á., Arnau, A., 2011. QCM technology in biosensors. Biosensors-Emerging Materials and Applications. InTech.

Muller, A., Neculoiu, D., Konstantinidis, G., Stavrinidis, A., Vasilache, D., Cismaru, A., Danila, M., Dragoman, M., Deligeorgis, G., Tsagaraki, K., 2009. 6.3-GHz film bulk acoustic resonator structures based on a gallium nitride/silicon thin membrane. IEEE Electron Device Letters 30(8), 799-801.

Nagaraju, M., Jingren, G., Lingley, A., Zhang, F., Small, M., Ruby, R., Otis, B., 2014. A fully integrated wafer-scale sub-mm 3 FBAR-based wireless mass sensor. Frequency Control Symposium (FCS), 2014 IEEE International, pp. 1-5. IEEE.

Nguyen, H., Park, J., Kang, S., Kim, M., 2015. Surface Plasmon Resonance: A Versatile Technique for Biosensor Applications. Sensors 15(5), 10481.

Nimse, S.B., Kim, T., 2013. Biological applications of functionalized calixarenes. Chemical Society Reviews 42(1), 366-386.

Nirschl, M., Blüher, A., Erler, C., Katzschner, B., Vikholm-Lundin, I., Auer, S., Vörös, J., Pompe, W., Schreiter, M., Mertig, M., 2009. Film bulk acoustic resonators for DNA and protein detection and investigation of in vitro bacterial S-layer formation. Sensors and Actuators A: Physical 156(1), 180-184.

Nirschl, M., Rantala, A., Tukkiniemi, K., Auer, S., Hellgren, A.C., Pitzer, D., Schreiter, M., Vikholm-Lundin, I., 2010. CMOS-integrated film bulk acoustic resonators for label-free biosensing. Sensors (Basel) 10(5), 4180-4193.

Ohno, R., Ohnuki, H., Wang, H., Yokoyama, T., Endo, H., Tsuya, D., Izumi, M., 2013. Electrochemical impedance spectroscopy biosensor with interdigitated electrode for detection of human immunoglobulin A. Biosensors and Bioelectronics 40(1), 422-426.

Paluch, G., Bartholomay, L., Coats, J., 2010. Mosquito repellents: a review of chemical structure diversity and olfaction. Pest management science 66(9), 925-935.

Pang, W., Zhao, H., Kim, E.S., Zhang, H., Yu, H., Hu, X., 2012. Piezoelectric microelectromechanical resonant sensors for chemical and biological detection. Lab Chip 12(1), 29-44.

Pashchenko, V., Matloub, R., Parsapourkolour, F., Muralt, P., Ballandras, S., Haffner, K., 2016. Hybrid BAW/SAW AlN and AlScN thin film resonator. Ultrasonics Symposium (IUS), 2016 IEEE International, pp. 1-4. IEEE.

Peluso, P., Wilson, D.S., Do, D., Tran, H., Venkatasubbaiah, M., Quincy, D., Heidecker, B., Poindexter, K., Tolani, N., Phelan, M., 2003a. Optimizing antibody immobilization strategies for the construction of protein microarrays. Analytical biochemistry 312(2), 113-124.

Peluso, P., Wilson, D.S., Do, D., Tran, H., Venkatasubbaiah, M., Quincy, D., Heidecker, B., Poindexter, K., Tolani, N., Phelan, M., Witte, K., Jung, L.S., Wagner, P., Nock, S., 2003b. Optimizing antibody immobilization strategies for the construction of protein microarrays. Analytical Biochemistry 312(2), 113-124.

Qin, L., Chen, Q., Cheng, H., Wang, Q.-M., 2010. Analytical study of dual-mode thin film bulk acoustic resonators (FBARs) based on ZnO and AlN films with tilted c-axis orientation. IEEE transactions on ultrasonics, ferroelectrics, and frequency control 57(8).

Qin, L., Wang, Q.-M., 2010. Mass sensitivity of thin film bulk acoustic resonator sensors based on polar c-axis tilted zinc oxide and aluminum nitride thin film. Journal of Applied Physics 108(10), 104510.

Qiu, X., Tang, R., Zhu, J., Oiler, J., Yu, C., Wang, Z., Yu, H., 2011. The effects of temperature, relative humidity and reducing gases on the ultraviolet response of ZnO based film bulk acoustic-wave resonator. Sensors and Actuators B: Chemical 151(2), 360-364.

Quan, J., Saaem, I., Tang, N., Ma, S., Negre, N., Gong, H., White, K.P., Tian, J., 2011. Parallel on-chip gene synthesis and application to optimization of protein expression. Nature Biotechnology 29(5), 449-452.

Quershi, A., Gurbuz, Y., Kang, W.P., Davidson, J.L., 2009. A novel interdigitated capacitor based biosensor for detection of cardiovascular risk marker. Biosens Bioelectron 25(4), 877-882.

Rey-Mermet, S., Lanz, R., Muralt, P., 2006. Bulk acoustic wave resonator operating at 8GHz for gravimetric sensing of organic films. Sensors and Actuators B: Chemical 114(2), 681-686.

Rodahl, M., Höök, F., Kasemo, B., 1996. QCM operation in liquids: an explanation of measured variations in frequency and Q factor with liquid conductivity. Analytical Chemistry 68(13), 2219-2227.

Rughoobur, G., DeMiguel-Ramos, M., Escolano, J.M., Iborra, E., Flewitt, A.J., 2017. Gravimetric sensors operating at 1.1 GHz based on inclined c-axis ZnO grown on textured Al electrodes. Sci Rep 7(1), 1367.

Rughoobur, G., DeMiguel-Ramos, M., Mirea, T., Clement, M., Olivares, J., Díaz-Durán, B., Sangrador, J., Miele, I., Milne, W.I., Iborra, E., Flewitt, A.J., 2016. Room temperature sputtering of inclined c-axis ZnO for shear mode solidly mounted resonators. Applied Physics Letters 108(3), 034103.

Sapsford, K.E., Ligler, F.S., 2004. Real-time analysis of protein adsorption to a variety of thin films. Biosens Bioelectron 19(9), 1045-1055.

Sauerbrey, G., 1959. Verwendung von Schwingquarzen zur Wägung dünner Schichten und zur Mikrowägung. Zeitschrift für Physik A Hadrons and Nuclei 155(2), 206-222.

Schramm, W., Paek, S.H., Voss, G., 1993. Strategies for the Immobilization of Antibodies. ImmunoMethods 3(2), 93-103.

Shons, A., Dorman, F., Najarian, J., 1972. An immunospecific microbalance. Journal of biomedical materials research 6(6), 565-570.

Singh, N.K., Jain, B., Annapoorni, S., 2011. ZnO modified gold disc: A new route to efficient glucose sensing. Sensors and Actuators B: Chemical 156(1), 383-387.

Singh, P., 2016. SPR Biosensors: Historical Perspectives and Current Challenges. Sensors and Actuators B: Chemical 229, 110-130.

Steichen, M., Brouette, N., Buess-Herman, C., Fragneto, G., Sferrazza, M., 2009. Interfacial Behavior of a Hairpin DNA Probe Immobilized on Gold Surfaces. Langmuir 25(7), 4162-4167.

Syed, Z., Leal, W.S., 2008. Mosquitoes smell and avoid the insect repellent DEET. Proceedings of the National Academy of Sciences 105(36), 13598-13603.

Tukkiniemi, K., Rantala, A., Nirschl, M., Pitzer, D., Huber, T., Schreiter, M., 2009. Fully integrated FBAR sensor matrix for mass detection. Procedia Chemistry 1(1), 1051-1054.

Vashist, S.K., Dixit, C.K., MacCraith, B.D., O'Kennedy, R., 2011. Effect of antibody immobilization strategies on the analytical performance of a surface plasmon resonance-based immunoassay. Analyst 136(21), 4431-4436.

Voiculescu, I., Nordin, A.N., 2012. Acoustic wave based MEMS devices for biosensing applications. Biosens Bioelectron 33(1), 1-9.

Wang, J., Chen, D., Xu, Y., Liu, W., 2014a. Label-free immunosensor based on micromachined bulk acoustic resonator for the detection of trace pesticide residues. Sensors and Actuators B: Chemical 190, 378-383.

Wang, W., Mayrhofer, P.M., He, X., Gillinger, M., Ye, Z., Wang, X., Bittner, A., Schmid, U., Luo, J., 2014b. High performance AlScN thin film based surface acoustic wave devices with large electromechanical coupling coefficient. Applied Physics Letters 105(13), 133502.

Wang, Z., Qiu, X., Chen, S.J., Pang, W., Zhang, H., Shi, J., Yu, H., 2011a. ZnO based film bulk acoustic resonator as infrared sensor. Thin Solid Films 519(18), 6144-6147.

Wang, Z., Qiu, X., Shi, J., Yu, H., 2011b. Room temperature ozone detection using ZnO based film bulk acoustic resonator (FBAR). Journal of The Electrochemical Society 159(1), J13-J16.

Weber, J., Albers, W.M., Tuppurainen, J., Link, M., Gabl, R., Wersing, W., Schreiter, M., 2006. Shear mode FBARs as highly sensitive liquid biosensors. Sensors and Actuators A: Physical 128(1), 84-88.

Wijaya, E., Lenaerts, C., Maricot, S., Hastanin, J., Habraken, S., Vilcot, J.-P., Boukherroub, R., Szunerits, S., 2011. Surface plasmon resonance-based biosensors: From the development of different SPR structures to novel surface functionalization strategies. Current Opinion in Solid State and Materials Science 15(5), 208-224.

Wingqvist, G., 2010. AlN-based sputter-deposited shear mode thin film bulk acoustic resonator (FBAR) for biosensor applications — A review. Surface and Coatings Technology 205(5), 1279-1286.

Wingqvist, G., Bjurstrom, J., Hellgren, A., Katardjiev, I., 2007. Immunosensor utilizing a shear mode thin film bulk acoustic sensor. Sensors and Actuators B: Chemical 127(1), 248-252.

Wingqvist, G., Yantchev, V., Katardjiev, I., 2008. Mass sensitivity of multilayer thin film resonant BAW sensors. Sensors and Actuators A: Physical 148(1), 88-95.

Wu, P., Hogrebe, P., Grainger, D.W., 2006. DNA and protein microarray printing on silicon nitride waveguide surfaces. Biosens Bioelectron 21(7), 1252-1263.

Xu, D., Liu, L., Guan, J., Xu, J., Wang, T., Qin, A., Hu, X., Wang, C., 2014. Label-free microcantilever-based immunosensors for highly sensitive determination of avian influenza virus H9. Microchimica Acta 181(3), 403-410.

Xu, H., Dong, S., Xuan, W., Farooq, U., Huang, S., Li, M., Wu, T., Jin, H., Wang, X., Luo, J., 2018. Flexible surface acoustic wave strain sensor based on single crystalline LiNbO3 thin film. Applied Physics Letters 112(9), 093502.

Xu, H., Zhao, X., Grant, C., Lu, J.R., Williams, D.E., Penfold, J., 2006. Orientation of a monoclonal antibody adsorbed at the solid/solution interface: a combined study using atomic force microscopy and neutron reflectivity. Langmuir 22(14), 6313-6320.

Xu, H., Zhao, X., Lu, J.R., Williams, D.E., 2007. Relationship between the structural conformation of monoclonal antibody layers and antigen binding capacity. Biomacromolecules 8(8), 2422-2428.

Xu, W., Appel, J., Chae, J., 2012. Real-Time Monitoring of Whole Blood Coagulation Using a Microfabricated Contour-Mode Film Bulk Acoustic Resonator. Journal of Microelectromechanical Systems 21(2), 302-307.

Xu, W., Zhang, X., Choi, S., Chae, J., 2011. A High-Quality-Factor Film Bulk Acoustic Resonator in Liquid for Biosensing Applications. Journal of Microelectromechanical Systems 20(1), 213-220.

Yakimova, R., Selegård, L., Khranovskyy, V., Pearce, R., Lloyd Spetz, A., Uvdal, K., 2012. ZnO materials and surface tailoring for biosensing. Frontiers in bioscience (Elite edition) 4(1), 254-278.

Yang, L., Li, Y., 2005. AFM and impedance spectroscopy characterization of the immobilization of antibodies on indium-tin oxide electrode through self-assembled monolayer of epoxysilane and their capture of Escherichia coli O157:H7. Biosens Bioelectron 20(7), 1407-1416.

Zhang, H., Marma, M.S., Bahl, S.K., Kim, E.S., McKenna, C.E., 2007. Sequence Specific Label-Free DNA Sensing Using Film-Bulk-Acoustic-Resonators. IEEE Sensors Journal 7(12), 1587-1588.

Zhang, H., Pang, W., Kim, E.S., Yu, H., 2010. Micromachined silicon and polymer probes integrated with film-bulk-acoustic-resonator mass sensors. Journal of Micromechanics and Microengineering 20(12), 125008.

Zhang, M., Cui, W., Liang, J., Zhang, D., Pang, W., Zhang, H., 2014a. A single-chip biosensing platform integrating FBAR sensor with digital microfluidic device. Ultrasonics Symposium (IUS), 2014 IEEE International, pp. 1521-1523. IEEE.

Zhang, M., Cui, W., Zhang, D., Pang, W., Zhang, H., 2014b. Response signal enhancement of film bulk acoustic Resonator mass sensor with bounded hydrophobic Teflon film. Frequency Control Symposium (FCS), 2014 IEEE International, pp. 1-4. IEEE.

Zhang, M., Du, L., Fang, Z., Zhao, Z., 2015a. Micro Through-hole Array in top Electrode of Film Bulk Acoustic Resonator for Sensitivity Improving as Humidity Sensor. Procedia Engineering 120, 663-666.

Zhang, M., Huang, J., Cui, W., Pang, W., Zhang, H., Zhang, D., Duan, X., 2015b. Kinetic studies of microfabricated biosensors using local adsorption strategy. Biosens Bioelectron 74, 8-15.

Zhang, R., Jiao, X.Q., Yang, J., Zhong, H., Shi, Y., 2014c. Electrode influence on effective electromechanical coupling coefficient of thin film bulk acoustic resonators. Materials Research Innovations 18(sup4), S4-606-S604-609.

Zhang, X., Xu, W., Abbaspour-Tamijani, A., Chae, J., 2009. Thermal Analysis and Characterization of a High Q Film Bulk Acoustic Resonator (FBAR) as Biosensers in Liquids. Micro Electro Mechanical Systems, 2009. MEMS 2009. IEEE 22nd International Conference on, pp. 939-942. IEEE.

Zhao, X., Ashley, G.M., Garcia-Gancedo, L., Jin, H., Luo, J., Flewitt, A.J., Lu, J.R., 2012a. Protein functionalized ZnO thin film bulk acoustic resonator as an odorant biosensor. Sensors and Actuators B: Chemical 163(1), 242-246.

Zhao, X., Pan, F., Ashley, G.M., Garcia-Gancedo, L., Luo, J., Flewitt, A.J., Milne, W.I., Lu, J.R., 2014. Label-free detection of human prostate-specific antigen (hPSA) using film bulk acoustic resonators (FBARs). Sensors and Actuators B: Chemical 190, 946-953.

Zhao, X., Pan, F., Cowsill, B., Lu, J.R., Garcia-Gancedo, L., Flewitt, A.J., Ashley, G.M., Luo, J., 2011. Interfacial immobilization of monoclonal antibody and detection of human prostate-specific antigen. Langmuir 27(12), 7654-7662.

Zhao, X., Pan, F., Garcia-Gancedo, L., Flewitt, A.J., Ashley, G.M., Luo, J., Lu, J.R., 2012b. Interfacial recognition of human prostate-specific antigen by immobilized monoclonal antibody: effects of solution conditions and surface chemistry. Journal of The Royal Society Interface 9(75), 2457-2467.

Zhao, X., Pan, F., Lu, J.R., 2009. Interfacial assembly of proteins and peptides: recent examples studied by neutron reflection. Journal of The Royal Society Interface, rsif20090168.

Zheng, D., Guo, P., Xiong, J., Wang, S., 2016a. Streptavidin Modified ZnO Film Bulk Acoustic Resonator for Detection of Tumor Marker Mucin 1. Nanoscale Research Letters 11(1), 396.

Zheng, D., Xiong, J., Guo, P., Li, Y., Wang, S., Gu, H., 2014. Detection of a carcinoembryonic antigen using aptamer-modified film bulk acoustic resonators. Materials Research Bulletin 59, 411-415.

Zheng, D., Xiong, J., Guo, P., Wang, S., Gu, H., 2016b. AlN-based film buck acoustic resonator operated in shear mode for detection of carcinoembryonic antigens. RSC Adv. 6(6), 4908-4913.

Zhu, C., Yang, G., Li, H., Du, D., Lin, Y., 2014. Electrochemical sensors and biosensors based on nanomaterials and nanostructures. Analytical chemistry 87(1), 230-249.